[57] L. Shu, K. L. Cheung, T. O. Khor, C. Chen, and A. N. Kong, "Phytochemicals: cancer chemoprevention and suppression of tumor onset and metastasis," *Cancer and Metastasis Reviews*, vol. 29, no. 3, pp. 483–502, 2010.

[58] Y. J. Surh, "NF-κB and Nrf2 as potential chemopreventive targets of some anti-inflammatory and antioxidative phytonutrients with anti-inflammatory and antioxidative activities," *Asia Pacific Journal of Clinical Nutrition*, vol. 17, no. 1, pp. 269–272, 2008.

[59] Y. J. Surh, J. K. Kundu, and H. K. Na, "Nrf2 as a master redox switch in turning on the cellular signaling involved in the induction of cytoprotective genes by some chemopreventive phytochemicals," *Planta Medica*, vol. 74, no. 13, pp. 1526–1539, 2008.

[60] Y. Miyagi, A. S. Om, K. M. Chee, and M. R. Bennink, "Inhibition of azoxymethane-induced colon cancer by orange juice," *Nutrition and Cancer*, vol. 36, no. 2, pp. 224–229, 2000.

[61] L. K. T. Lam, J. Zhang, S. Hasegawa, and H. A. J. Schut, "Inhibition of chemically induced carcinogenesis by citrus limonoids," in *Food Phytochemicals for Cancer Prevention I. Fruits and Vegetables*, M. T. Huang, T. Osawa, C. T. Ho, and R. T. Rosen, Eds., pp. 209–219, American Chemical Society, Washington, DC, USA, 1994.

[62] O. S. Sohn, E. S. Fiala, S. P. Requeijo, J. H. Weisburger, and F. J. Gonzalez, "Differential effects of CYP2E1 status on the metabolic activation of the colon carcinogens azoxymethane and methylazoxymethanol," *Cancer Research*, vol. 61, no. 23, pp. 8435–8440, 2001.

[63] M. D. M. Von Pressentin, K. El-Bayoumy, and J. B. Guttenplan, "Mutagenic activity of 4-nitroquinoline-N-oxide in upper aerodigestive tissue in lacZ mice (Muta(TM)Mouse) and the effects of 1,4- phenylenebis(methylene)selenocyanate," *Mutation Research*, vol. 466, no. 1, pp. 71–78, 2000.

[64] Z. Serefoglou, C. Yapijakis, E. Nkenke, and E. Vairaktaris, "Genetic association of cytokine DNA polymorphisms with head and neck cancer," *Oral Oncology*, vol. 44, no. 12, pp. 1093–1099, 2008.

[65] B. Raju and S. O. Ibrahim, "Pathophysiology of oral cancer in experimental animal models: a review with focus on the role of sympathetic nerves," *Journal of Oral Pathology and Medicine*, vol. 40, no. 1, pp. 1–9, 2011.

[66] T. Tanaka, H. Kohno, M. Murakami, R. Shimada, and S. Kagami, "Colitis-related rat colon carcinogenesis induced by 1-hydroxyanthraquinone and methylazoxymethanol acetate (review)," *Oncology Reports*, vol. 7, no. 3, pp. 501–508, 2000.

[67] D. W. Rosenberg, C. Giardina, and T. Tanaka, "Mouse models for the study of colon carcinogenesis," *Carcinogenesis*, vol. 30, no. 2, pp. 183–196, 2009.

[68] B. H. Cohen, E. L. Diamond, C. G. Graves et al., "A common familial component in lung cancer and chronic obstructive pulmonary disease," *The Lancet*, vol. 2, no. 8037, pp. 523–526, 1977.

[69] T. Kawamori, T. Tanaka, Y. Hirose, M. Ohnishi, and H. Mori, "Inhibitory effects of d-limonene on the development of colonic aberrant crypt foci induced by azoxymethane in F344 rats," *Carcinogenesis*, vol. 17, no. 2, pp. 369–372, 1996.

[70] T. Tanaka, K. Kawabata, M. Kakumoto et al., "Citrus auraptene exerts dose-dependent chemopreventive activity in rat large bowel tumorigenesis: the inhibition correlates with suppression of cell proliferation and lipid peroxidation and with induction of phase II drug- metabolizing enzymes," *Cancer Research*, vol. 58, no. 12, pp. 2550–2556, 1998.

[71] T. Tanaka, Y. Yasui, R. Ishigamori-Suzuki, and T. Oyama, "Citrus compounds inhibit inflammation- and obesity-related colon carcinogenesis in mice," *Nutrition and Cancer*, vol. 60, no. 1, pp. 70–80, 2008.

[72] T. Tanaka, H. Makita, K. Kawabata et al., "Chemoprevention of azoxymethane-induced rat colon carcinogenesis by the naturally occurring flavonoids, diosmin and hesperidin," *Carcinogenesis*, vol. 18, no. 5, pp. 957–965, 1997.

[73] T. Tanaka, M. Maeda, H. Kohno et al., "Inhibition of azoxymethane-induced colon carcinogenesis in male F344 rats by the citrus limonoids obacunone and limonin," *Carcinogenesis*, vol. 22, no. 1, pp. 193–198, 2001.

[74] A. Murakami, K. Wada, N. Ueda et al., "In Vitro absorption and metabolism of a citrus chemopreventive agent, auraptene, and its modifying effects on xenobiotic enzyme activities in mouse livers," *Nutrition and Cancer*, vol. 36, no. 2, pp. 191–199, 2000.

Mutation Research 748 (2012) 29–35

Contents lists available at SciVerse ScienceDirect

Mutation Research/Genetic Toxicology and Environmental Mutagenesis

journal homepage: www.elsevier.com/locate/gentox
Community address: www.elsevier.com/locate/mutres

Dammar resin, a non-mutagen, inducts oxidative stress and metabolic enzymes in the liver of *gpt* delta transgenic mouse which is different from a mutagen, 2-amino-3-methylimidazo[4,5-*f*]quinoline

Xiao-Li Xie, Min Wei, Anna Kakehashi, Shotaro Yamano, Kyoko Okabe, Masaki Tajiri, Hideki Wanibuchi*

Department of Pathology, Osaka City University Graduate School of Medicine, Asahi-machi 1-4-3, Abeno-ku, 545-8585 Osaka, Japan

ARTICLE INFO

Article history:
Received 28 February 2012
Received in revised form 6 June 2012
Accepted 23 June 2012
Available online 6 July 2012

Keywords:
Dammar resin
IQ
Genotoxicity
Oxidative stress
Cytochrome P450s

ABSTRACT

Dammar resin has long been used in foods as either a clouding or a glazing agent. In a recent study, 2% Dammar resin showed significant hepatocarcinogenicity in a rat 2-year bioassay. Therefore, for an accurate estimate of human risk, it is necessary to understand whether Dammar resin induces liver genotoxicity and the underlying mechanisms of its hepatocarcinogenicity. Modifying effects of 2-amino-3-methylimidazo[4,5-*f*]quinoline (IQ), a typical genotoxic carcinogen produced during cooking of protein-rich foods, was also studied in the present study. Exposure of *gpt* delta mice to Dammar resin at a dose of 2% for 12 weeks did not induce any obvious mutagenicity in the liver. However, the index of cell proliferation, the level of 8-OHdG, and *bax*, *bcl-2*, *p53*, *cyp1a2*, *cyp2e1*, *gpx1* and *gstm2* gene expression were all significantly increased when compared with the control group. In the IQ treatment group, at a dose of 300 ppm, mutagenicity was readily detected, the index of cell proliferation increased, and *p53*, *cyp2e1* and *gpx1* gene expression was down-regulated in the liver. Down-regulation of *p53*, *P450s*, and *gpx1* in the livers of IQ treated mice are consistent with its genotoxic mechanism of carcinogenicity observed in a 675-day study. In contrast, our results using *gpt* delta mice suggest that Dammar resin is not genotoxic. Instead, the Dammar resin-induced hepatocarcinogenicity seen in our previous 2-year study with rats may have been mediated by non-genotoxic mechanisms, including increased P450 enzyme activity, increased oxidative stress, altered gene expression, and promotion of cell proliferation.

© 2012 Elsevier B.V. All rights reserved.

1. Introduction

Carcinogens can be classified into two categories, genotoxic and non-genotoxic. The former indicates a chemical capable of producing cancer by directly causing irreversible genetic damage, while the latter represents a chemical capable of producing cancer by some secondary mechanisms not related to direct gene damage [1].

Heterocyclic aromatic amines are the major class of genotoxic hepatocarcinogens in rodents [2]. 2-amino-3-methylimidazo[4,5-*f*]quinoline (IQ) is a genotoxic and carcinogenic heterocyclic amine formed by high-temperature cooking of proteinaceous food [2,3]. Long-term treatment (675 days) with 300 ppm IQ has been shown to induce tumors in the liver, lung and forestomach of CDF1 mice [4]. The In vivo mutagenicity and the mutation spectrum of IQ has been examined in commercially available transgenic rodent models such as BigBlue and guanine phosphoribosyltransferase (*gpt*) transgenic rats [3,5]. On the basis of these results, IQ was chosen as a positive mutagen for mutation assays.

Currently, little is known about Dammar resin metabolism. Dammar resin, isolated from plants belonging to the family Dipterocarpaceae, contains dammarane type triterpenes [6], which was reported to possess antiviral activities and to be protective against in vitro low density lipoprotein (LDL) oxidation [6,7]. Dammar resin is widely used in the food industry as a stabilizer and thickener. However, in a rat 2-year bioassay, the incidence of liver tumors was significantly increased in rats administered 2% Dammar resin when compared with the control group (unpublished data). The mechanism by which it exerts carcinogenic activity in rats has not been fully clarified.

The capability of a carcinogen to directly induce genetic mutations is routinely evaluated. However, in a recent study, up to 90% of rodent non-carcinogens tested positive in one or more of the standard in vitro assays used to determine the mutagenic capability of potential carcinogens, resulting in an unacceptably high number of false positive results [8]. Therefore, an in vivo genotoxicity test of Dammar resin and exploration of its mechanisms of hepatocarcinogenicity are required to help to evaluate the risk of this potential human carcinogen.

* Corresponding author. Tel.: +81 6 6645 3735; fax: +81 6 6646 3093.
E-mail address: wani@med.osaka-cu.ac.jp (H. Wanibuchi).

1383-5718/$ – see front matter © 2012 Elsevier B.V. All rights reserved.
http://dx.doi.org/10.1016/j.mrgentox.2012.06.005

8-hydroxydeoxyguanosine (8-OHdG) is well established as a representative biomarker for oxidative stress [9]: Oxidative damage to DNA is considered to be important in the mutagenesis and carcinogenesis process. The cytochrome P450s (P450s) act on a wide variety of chemicals, and their involvement in the production of reactive oxygen species during substrate oxidation is well documented [10,11]. Various chemicals with P450-inducible properties demonstrate hepatocarcinogenicity without overt genotoxicity [12–14], which suggests that reactive oxygen species resulting from increased activity of P450s enzymes may play a role in the carcinogenic activity of these chemicals. Researchers have hypothesized that non-genotoxic hepatocarcinogens with P450-inducible capability may cause oxidative damage to liver DNA, which might subsequently take part in inducing carcinogenesis [15].

The *gpt* delta mouse was established by microinjection of λ EG10 phage DNA (48 kb) into the fertilized eggs of C57BL/6J mice [16]. Progeny, carrying 80 copies of the transgene in a head-to-tail fashion at a single site of chromosome 17, were obtained and are maintained as homozygotes. These homozygous mice have been useful in the assessment of the in vivo genotoxicity and the estimation of carcinogenic risk of environmental chemicals [17].

In the present study, the in vivo genotoxicity of Dammar resin and IQ were examined using *gpt* delta mice and their possible mechanisms of hepatocarcinogenicity are discussed.

2. Materials and methods

2.1. Animals, diet and housing conditions

Eighteen male 5-week-old *gpt* delta C57BL/6J transgenic mice were obtained from Japan SLC and housed in plastic cages (six animals/cage) in our animal facility; animals were maintained under standard conditions (room temperature, 23 ± 1 °C; relative humidity, 44 ± 5%; and light/dark cycle, 12 h) and given free access to powdered diet (Oriental MF; Oriental Yeast, Tokyo, Japan) and tap water. Dammar resin was kindly provided by San-Ei Gen F.F.I., Inc., Osaka, Japan. The animals were acclimatized for 1 week prior to beginning the experiment. The experiment was conducted following approval of the Animal Care and Use Committee of the Osaka City University Graduate School of Medicine.

2.2. Animal treatments

Eighteen *gpt* delta transgenic mice were randomly divided into three groups (6 in each group) and were fed a basal diet or diet containing 2% Dammar resin or 300 part per million (ppm) of IQ for 12 weeks followed by 2-week basal diet, as described previously [18]. The dose levels of Dammar resin and IQ used in the present study are consistant with the carcinogenic levels which were studied in previous long-term carcinogenesis studies. In the present study, 12 weeks feeding with Dammar resin or IQ followed by a 2-week treatment-free period was employed because in previous transgenic studies using the *gpt* delta transgenic mouse [18,19], a positive response could be readily detected after a 12-week exposure to genotoxic carcinogens, and, in transgenic assays, it is important to choose an appropriate expression time, i.e., the time after the last exposure to mutagen which is required for the mutant frequency to stabilize in a given tissue [20]. An appropriate expression time for liver is 14 days [21].

All surviving animals were killed under deep anesthesia at the end of the experiment. The livers were isolated from each animal and immediately excised, weighted, and dissected into halves. One half was immediately frozen in liquid nitrogen and stored at −80 °C for mutation assays and gene expression analyses. The other half was cut into 2–3-mm thick slices. The slices were fixed in 10% buffered formalin solution and routinely processed to paraffin blocks for histopathological examination and immunohistochemistry. Hematoxylin and eosin (H&E)-stained tissue cut from the blocks were examined by light microscopy.

2.3. Immunohistochemistry staining for ki-67

Paraffin blocks of the livers were sectioned at 3-μm thickness. After deparaffinization, sections were incubated with 30% hydrogen peroxide to block endogenous peroxidase and antigen retrieval was performed by microwaving at 95 °C for 30 min. After blocking, sections were incubated with ki-67 primary antibody (1:500, 550690, BD Pharmingen, USA) overnight at 4 °C. Antigen visualization was done with 3,3′-diaminobenzidine tetrahydrochloride (DAB). To investigate proliferative activity, at least 1000 hepatocyte nuclei were counted in each liver; labeling indices were calculated as the percentage of cells positive for ki-67 staining.

2.4. Measurement of 8-OHdG

Nuclear DNA was extracted with a DNA Extractor WB kit (Wako Pure Chemical Industries) containing an antioxidant NaI solution to dissolve cellular components. For additional prevention of auto-oxidation in the cell lysis step, deferoxamine mesylate (Sigma Chemical, St Loius, MO, USA) was added to the lysis buffer. The DNA was digested into deoxynucleotides by treatment with nuclease P1 (Yamasa Shoyu, Chiba, Japan) and alkaline phosphatase (Sigma Chemical), and levels of 8-OHdG (8-OHdG/10^5 dG) were measured by high-performance liquid chromatography with an electrochemical detection system (Coulochem II; ESA, Bedford, MA, USA).

2.5. DNA isolation and in vitro packaging of λ phage DNA

High-molecular-weight genomic DNA was extracted from liver tissue using the RecoverEase DNA Isolation kit (Stratagene, La Jolla, CA, USA). λ EG10 phages were rescued using Transpack Packaging Extract (Stratagene).

2.6. gpt mutation assay

The assay was conducted according to previously published methods [16]. All the confirmed *gpt* mutants recovered from the livers were sequenced; identical mutations from the same mouse were counted as one mutant. The mutant frequency (MF) of the *gpt* gene in the liver was calculated by dividing the number of confirmed 6-thioguanine (6-TG)-resistant colonies by the number of rescued plasmids. DNA sequencing of the *gpt* gene was performed with the BigDye Terminater Cycle Sequencing Ready Reaction (Applied Biosystems, Inc., Carlsbad, CA, USA) on an Applied Biosystems PRISM 310 Genetic Analyzer.

2.7. Spi⁻ assay

The Spi⁻ assay was conducted according to previously published methods [16]. Packaged phages were incubated with *E. coli* XL-1 Blue MRA for survival titration and *E. coli* XL-1 Blue MRA P2 for mutant selection. Infected cells were mixed with molten lambda-trypticase agar plates. The next day, plaques (Spi⁻ candidates) were punched out with sterilized glass pipettes and the agar plugs were suspended in SM buffer. The Spi⁻ phenotype was confirmed by spotting the suspensions on three types of plates in which XL-1 Blue MRA, XL-1 Blue MRA P2, or WL95 P2 strains were spread with soft agar. True Spi⁻ mutants, which made clear plaques on all of the plates, were counted. Spi⁻ mutant lysates were obtained by infecting E. coli LE392with the recovered Spi⁻ mutants.

2.8. Quantitative real-time reverse transcription-polymerase chain reaction (RT-PCR) analysis of p53, bax, bcl-2, caspase-3, cyp1a1, cyp1a2, cyp2e1, cyp2r1, cyp7b1, glutathione peroxidase 1 (gpx1) and glutathion S-transferase mu 2 (gstm2) mRNA

Total RNA was extracted with TRIzol Reagent (Invitrogen) according to the manufacturer's instructions. cDNA copies of total RNA were obtained using a High Capacity cDNA Reverse Transcription kit (Applied Biosystems Japan Ltd.). Primers and probes (Taqman Gene Expression Assay) were purchased from Applied Biosystems, Inc., Carlsbad, CA, USA. The PCR program cycles were set as follows: initial denaturing at 95 °C for 20 s, followed by 40 cycles at 95 °C for 3 s, and 60 °C for 30 s. PCR reactions were performed as described previously [22], with primers for mouse *p53*, *bax*, *bcl-2*, *caspase-3*, *cyp1a1*, *cyp1a2*, *cyp2e1*, *cyp2r1*, *cyp7b1*, *gpx1* and *gstm2*. β-Actin mRNA was employed as an internal standard, and the mRNA levels of the target gene were normalized to the β-actin mRNA level. The Values in each treatment group were expressed as fold increases compared to the mean value in the control group, which was given an arbitrary value of 1.

2.9. Statistical analysis

All mean values were expressed as the mean ± standard deviation (SD). Statistical analyses were performed using the Statlight program (Yukms Co., Ltd., Tokyo, Japan). Homogeneity of variance was tested by the F test between the treatment and control groups. Differences in mean values between the treatment and control groups were evaluated by the two-tailed Student's *t*-test when variance was homogeneous and the two-tailed Aspin–Welch *t*-test when variance was heterogeneous. *p* values less than 0.05 were considered significant.

3. Results

3.1. Body and liver weights, water intake, food consumption and compound intake

The results for body and liver weights, water intake, food consumption and compound intake of the mice are presented in Table 1. In the Dammar resin group, one mouse died during the

Table 1
Final body weight, liver weight, water intake, food consumption and compounds intake of *gpt* delta transgenic mice.

Groups Number of effective mice	Control 6	2% Dammar resin 5	300 ppm IQ 6
Final body weight (g)	34.67 ± 1.87	28.76 ± 0.09*	30.7 ± 1.27*
Absolute liver weight (g)	1.20 ± 0.13	1.06 ± 0.08	1.38 ± 0.09*
Relative liver weight (g/g body weight)	0.035 ± 0.005	0.037 ± 0.003	0.045 ± 0.002*
Average water intake (g/g body weight/day)	0.24 ± 0.05	0.22 ± 0.03	0.26 ± 0.02
Average food intake (g/g body weight/day)	0.13 ± 0.02	0.12 ± 0.02	0.13 ± 0.02
Average compound intake (mg/g body weight/day)	-	2.43 ± 0.32	0.04 ± 0.01

* $p < 0.05$ versus the control group.

second week. Since the cause of death was unclear, it was not included in the final analysis.

Dammar resin and IQ did not affect average water or food intake, but significantly suppressed final body weight. No significant changes of absolute or relative liver weights were observed in the Dammar resin-treated group. The absolute and relative liver weights were significantly increased in the IQ-treated group ($p < 0.05$).

3.2. Histopathological evaluation and hepatocyte proliferation analysis

There were no obvious pathologic changes in the livers of the Dammar resin group; hypertrophy and vacuolar degeneration of hepatocytes were observed in some livers of IQ-treated mice (data not shown).

Fig. 1 shows the results of cell proliferation analysis by ki-67 staining. Proliferation of hepatocytes was significantly elevated in both Dammar resin and IQ treatment groups compared with the control group.

3.3. Examination of oxidative stress by 8-OHdG measurement

Fig. 2 shows the 8-OHdG levels in the livers. Significant increases of 8-OHdG were present in the Dammar resin-treated group, but not in the IQ treatment group, compared with the control group.

3.4. In vivo mutation assay

Data for *gpt* MF analyzed by 6-TG selection are summarized in Table 2. There was no difference in the *gpt* MF in the Dammar resin-treated mice (3.01×10^{-6}) compared with the control group (5.39×10^{-6}). In contrast, in the IQ-treated mice, *gpt* MF (32.49×10^{-6}) was significantly increased, approximately 6-fold higher than the control group.

To characterize the *gpt* mutations in the livers, DNA sequencing was performed (Table 3). In Dammar resin-treated mice, the predominant types of base substitutions were G:C to A:T transitions (5/12 = 41.7%) and G:C to T:A transversions (3/12 = 25%), neither of which differed significantly from the control group. On the other hand, the predominant type of base substitution in the IQ treatment group was the G:C to T:A transversion (81/117 = 69.2%), which was significantly increased compared to the control group.

The results of the Spi^- mutation assay are shown in Table 4. There was no difference in Spi^- mutant frequency in the mice administered Dammar resin (5.94 ± 3.00, $p > 0.05$), but Spi^- mutant frequency in mice fed IQ (21.69 ± 10.44, $p < 0.01$) is significantly elevated compared to the control (6.21 ± 1.05).

3.5. mRNA expression levels of p53, bax, bcl-2, caspase-3, cyp1a1, cyp1a2, cyp2e1, cyp2r1, cyp7b1, gpx1 and gstm2 in mouse liver

RT-PCR was performed on all the mice livers. The results are shown in Fig. 3. Expression of *p53*, *bax*, *bcl-2*, *cyp1a2*, *cyp2e1*, *gpx1* and *gstm2* were significantly increased in Dammar resin-treated mice ($p < 0.05$). Expression of *p53*, *cyp2e1* as well as *gpx1* were

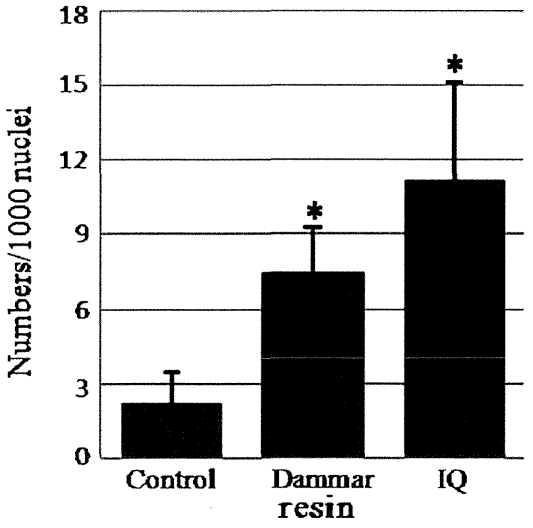

Fig. 1. Cell proliferation index. Compared with the control group, hepatocyte proliferation was significantly elevated by administeration of Dammar resin or IQ, at doses of 2% and 300 ppm, respectively. Significant compared with the control group (*$p < 0.05$).

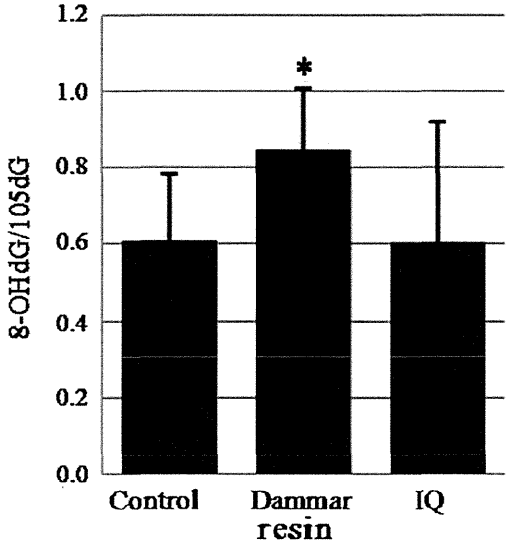

Fig. 2. Formation of 8-OHdG in the liver. The level of 8-OHdG was significantly increased by treatment with 2% Dammar resin, while no change was observed with 300 ppm IQ treatment. Significant compared with the control group (*$p < 0.05$).

Table 2
gpt mutation frequency in mouse livers.

Treatment	Mouse number	Cm^R colonies ($\times 10^5$)	Independent *gpt* mutation	*gpt* MF ($\times 10^{-6}$)	Mean ± SD
Control	11	7.80	3	3.85	5.39 ± 2.78
	12	7.08	4	5.65	
	13	7.29	3	4.12	
	14	6.27	6	9.57	
	15	5.64	1	1.77	
	16	5.40	4	7.41	
2% Dammar resin	21	9.60	2	2.08	3.01 ± 1.19
	22	5.52	1	1.81	
	23	7.48	2	2.67	
	24	5.10	2	3.92	
	26	10.96	5	4.56	
300 ppm IQ	31	6.51	14	21.51	32.49 ± 11.14*
	32	5.13	19	37.04	
	33	6.99	22	31.47	
	34	6.99	17	24.32	
	35	6.36	18	28.30	
	36	5.16	27	52.33	

* $p < 0.01$ versus the control group.

Table 3
Classification of *gpt* mutations in *gpt* delta mouse livers.

Types of *gpt* mutation	Control		2% Dammar resin		300 ppm IQ	
	Number (%)	Mutant frequency ($\times 10^{-6}$)	Number (%)	Mutant frequency ($\times 10^{-6}$)	Number (%)	Mutant frequency ($\times 10^{-6}$)
Base substitution						
Transition						
G:C to A:T	3(14.3)	0.71 ± 0.79	5(41.7)	1.18 ± 1.19	8(6.8)	2.25 ± 1.80
A:T to G:C	2(9.5)	0.49 ± 0.77	1(8.3)	0.39 ± 0.88	3(2.6)	0.76 ± 1.30
Transversion						
G:C to T:A	5(23.8)	1.25 ± 1.07	3(25)	0.68 ± 0.97	81(69.2)	22.56 ± 7.17*
G:C to C:G	1(4.8)	0.24 ± 0.58	0	0 ± 0	7(6)	1.92 ± 2.53
A:T to T:A	0	0 ± 0	0	0 ± 0	2(1.7)	0.65 ± 1.59
A:T to C:G	2(9.5)	0.57 ± 0.89	0	0 ± 0	1(0.9)	0.26 ± 0.64
Deletion						
Single bp	2(9.5)	0.45 ± 0.70	0	0 ± 0	6(5.1)	1.65 ± 1.83
Over 2bp	1(4.8)	0.31 ± 0.76	0	0 ± 0	2(1.7)	0.49 ± 0.77
Insertion	5(23.8)	1.36 ± 1.70	2(16.7)	0.57 ± 0.87	6(5.1)	1.63 ± 1.59
Others	0	0 ± 0	1(8.3)	0.18 ± 0.41	1(0.9)	0.32 ± 0.79
Total	21(100)	5.39 ± 2.78	12(100)	3.01 ± 1.19	117(100)	32.49 ± 11.14*

* $p < 0.01$ versus the control group.

significantly decreased in IQ-treated mice ($p < 0.05$). The ratio of *bax* versus *bcl-2* as well as expression of *caspase-3*, *cyp1a1*, *cyp2r1* and *cyp7b1* did not differ in the treated groups compared with the control group.

4. Discussion

IQ is known to be a potent mutagen for the liver [23], and it was therefore used as a positive control mutagen for validating

Table 4
Spi^- mutant frequency in mouse livers.

Treatment	Mouse number	Plaques within XL-1 Blue MRA ($\times 10^5$)	Plaque within WL95 (P2)	Mutant frequency ($\times 10^{-6}$)	Mean ± SD
Control	11	13.06	6	4.59	6.21 ± 1.05
	12	10.22	7	6.85	
	13	11.24	7	6.23	
	14	10.58	8	7.56	
	15	10.92	6	5.49	
	16	24.39	16	6.56	
2% Dammar resin	21	15.96	4	2.51	5.94 ± 3.00
	22	13.72	13	9.48	
	23	14.44	6	4.16	
	24	10.38	9	8.67	
	26	10.18	5	4.91	
300 ppm IQ	31	10.16	15	14.76	21.69 ± 10.44*
	32	12.24	20	16.34	
	33	14.26	49	34.36	
	34	14.12	29	20.54	
	35	21.68	21	9.69	
	36	11.04	38	34.42	

* $p < 0.01$ versus the control group.

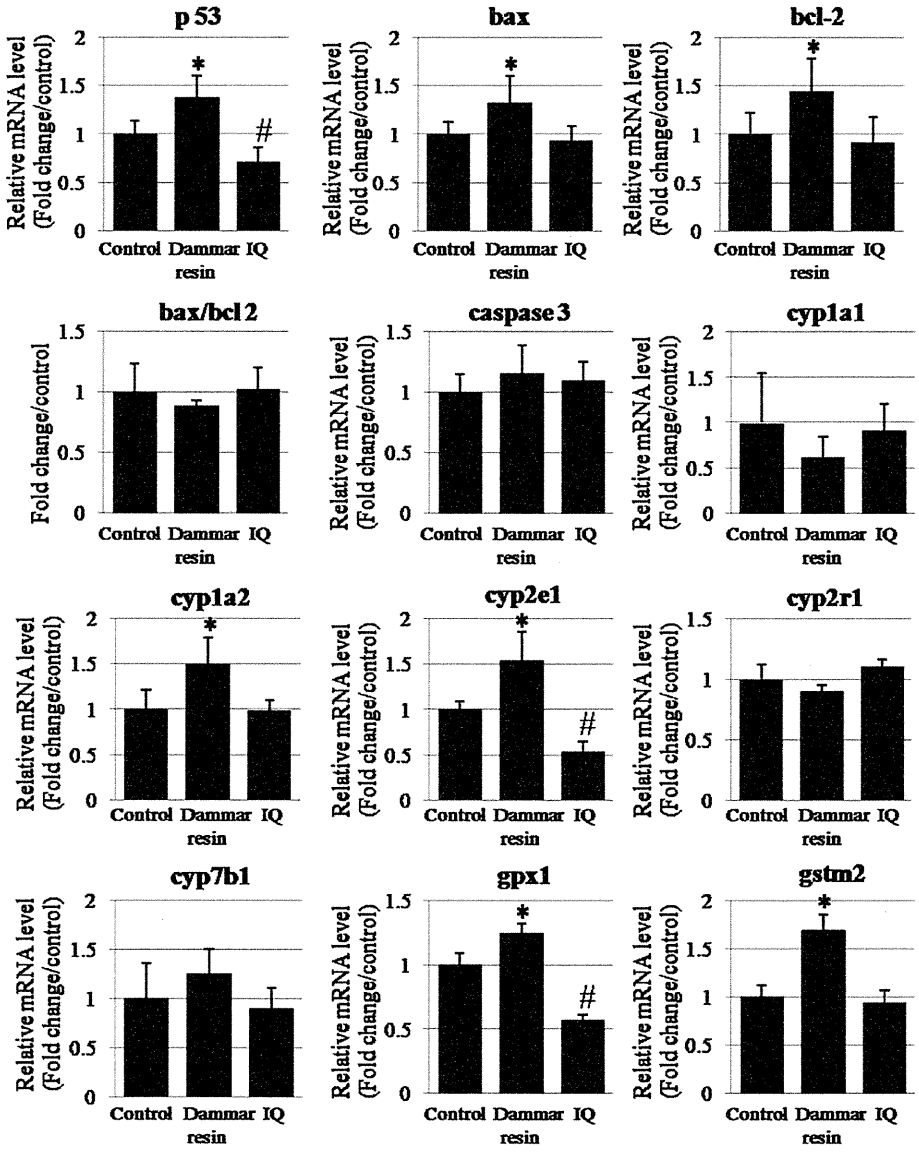

Fig. 3. mRNA expression of *p53*, *bax*, *bcl-2*, *bax/bcl-2*, *caspase-3*, *cyp1a1*, *cyp1a2*, *cyp2e1*, *cyp2r1*, *cyp7b1*, *gpx1* and *gstm2* in the livers of *gpt* delta mice. Significantly increased *p53*, *bax*, *bcl-2*, *cyp1a2*, *cyp2e1*, *gpx1* and *gstm2* gene expression was observed in the Dammar resin-treated group, while significantly decreased *p53*, *cyp2e1* and *gpx1* gene expression was observed in the IQ-administered group. The ratio of *bax* versus *bcl-2* as well as the mRNA expression of *caspase-3*, *cyp1a1*, *cyp2r1* and *cyp7b1* did not differ in the treated and control groups. Significantly up-regulated compared with the control group ($^{*}p < 0.05$); significantly down-regulated compared with the control group ($^{\#}p < 0.05$).

the mutagenicity assay system. In the present study, the mutation assay clearly showed that exposure to IQ at a dose of 300 ppm for 12 weeks was mutagenic. Significant increases in *gpt* MF, for the detection of point mutations, and Spi$^-$ MF, mainly attributable to deletion mutations, were found in IQ-treated mice. In the *gpt* assay, IQ primarily caused transversion of G:C to T:A, which is consistent with previous studies [3,5].

On the other hand, exposure to Dammar resin at a dose of 2% for 12 weeks was not mutagenic, which was consistent with the results of our mutation assay conducted in *gpt* delta transgenic rats (manuscript in preparation). There was no change in either the *gpt* MF or Spi$^-$ MF between the Dammar resin and control group. In the Dammar resin-administered group, the predominant types of base substitutions were G:C to A:T transitions and G:C to T:A transversions, neither of which were significantly different from the control group.

Ki-67 is a nuclear marker of cell proliferation and is detectable in the cell at all phases of the cell cycle except G_0 [24]. The ki-67 labeling index is associated with liver cancer outcome [25]. In the present study, proliferation of hepatocytes was significantly augmented by administration of both IQ and Dammar resin, suggesting the possibility that enhanced cell proliferation might be at least partly responsible for the carcinogenic activity of these agents.

Oxidative DNA damage with 8-OHdG formation is reported to be induced by 2-amino-imidazo[4,5-*f*]quinoline [23] and is thought to play a critical role in IQ-mediated carcinogenesis. However, in the present study, IQ did not induce 8-OHdG formation. Our result was consistent with the studies of Kitamura et al. [26] and Wei et al. [22]: the level of 8-OHdG was not significantly changed in the livers of rats treated with 300 ppm IQ.

It is generally recognized that oxidative stress occurs in a cell or tissue when the concentration of reactive oxygen species (ROS)

generated exceeds the antioxidant capability of that cell [27]. ROS generation is related to P450 enzyme activity. Multiple sources of ROS may contribute to persistent oxidative stress, resulting in higher 8-OHdG levels, and subsequently resulting in pathophysiologic changes that allow for the selective growth of preneoplastic initiated cells [27]. In the present study, levels of P450 enzymes and 8-OHdG levels were increased in the Dammar resin fed group, suggesting that Dammar resin may induce the expression and activity of P450 enzymes which would result in increased ROS production and 8-OHdG generation. However, while the Dammar resin fed group had increased 8-OHdG levels, there was no evidence suggestive of direct DNA damage, i.e., the Dammar resin fed group did not have increased DNA mutations. Therefore, our results suggest that the production of reactive oxygen species resulting from increased expression and activity of P450 enzymes, while causing chemical damage to DNA bases, is insufficient to cause permanent gene mutations; this result is consistent with a previous study [15].

Disruption of apoptosis can promote tumor initiation and progression [28], and the induction of apoptosis is central to the tumor-suppressive activity of p53 [29]. Bax is a proapoptotic Bcl-2 family member that binds to the anti-apoptotic Bcl-2 protein and antagonizes its function [30]. The *bax* gene is known to be transcriptionally regulated by p53 during induction of apoptosis [31,32]. Thus, up-regulated *bax* is one mechanism whereby p53 induces apoptosis [33]. Furthermore, p53 loss and Bcl-2 overexpression can have virtually identical effects on the pathology of some tumors [34]. Caspase-3 is a key mediator of apoptosis and can be activated through both extrinsic and intrinsic signaling pathways [35,36]. In the present study, treatment with IQ significantly down-regulated expression of *p53* expression, but did not affect expression of *bax*, *bcl-2* or *caspase-3* or change the ratio of *bax* versus *bcl-2*. Treatment with Dammar resin significantly increased expression of *p53*, *bax* and *bcl-2* genes, but did not change the ratio of *bax* versus *bcl-2* or change expression of *caspase-3*. This suggests that neither IQ nor Dammar resin affected basal apoptotic/anti-apoptotic signaling in hepatocytes, but expression of *p53*, the upstream inhibitor of *bcl-2* and activator of apoptosis [34], was affected by these agents: IQ suppressed expression of *p53* mRNA while Dammar resin induced expression of *p53* mRNA. This suggests that in the livers of *gpt* delta mice, the genotoxic agent IQ suppresses apoptotic removal of mutated cells with carcinogenic potential while the non-genotoxic agent Dammar resin does not suppress apoptotic removal of cells with carcinogenic potential. This also explains why Dammar resin increased the formation of 8-OHdG but did not cause an increase in mutation frequency in the livers of Dammar resin treated mice.

P450s are the predominant catalysts of phase I metabolism in the liver. It has been generally accepted that the various forms of P450s show different rates of activation as well as detoxication of chemical carcinogens [37]. Gpx1 is a phase II enzyme: Gpx1 is one of the most important of the antioxidant phase II metabolic enzymes which protect cells and tissues from damage caused by reactive oxygen species by helping to maintain the balance between prooxidant and antioxidant forces [38]. Gstm2 is another phase II enzyme: Gstm2 is a member of the Glutathione S-transferase (GST) family which represents a major group of detoxification enzymes [39].

In our study, mRNA levels of *cyp2e1* were significantly down-regulated by treatment with IQ. In addition, IQ itself is able to affect the activity of P450s enzymes depending on the treatment regimen [40]. Low P450s enzyme activity would delay the metabolic conversion of IQ into a substrate for GST enzymes and this may be one factor in the low mRNA levels of *gpx1* after treatment with IQ. Morgan et al. [41] suggest that low levels of P450s mRNA and proteins in tumor-bearing mice and repression of hepatic transport proteins is linked with reduced drug clearance and the resultant toxicity of the drug. Taken together, these data suggest that the delay of metabolic transformation of IQ and its metabolites may be involved in its toxicity.

In the Dammar resin treatment group, mRNA levels of *cyp1a2*, *cyp2e1*, *gpx1* and *gstm2* were significantly up-regulated compared to the control group. While induction of detoxification and antioxidant enzymes (*gpx1* and *gstm2*) is protective [41,42], induction of these enzymes also indicates production of reactive metabolites by phase I enzymes. Importantly, induction of P450s by chemicals can induce hepatocarcinogenicity in rodents without overt genotoxicity [13,14]. Induction of P450s (*cyp1a2* and *cyp2e1*) by Dammar resin administration might play a role in carcinogenicity through mechanisms related to oxidative stress [43]: Klaunig et al. [27] have shown that chronic sublethal oxidative injury can alter cellular metabolic pathways and gene expression, leading to altered cell growth in the absence of genetic mutations. Thus, we hypothesize that intranuclear oxidative stress could play a role in Dammar resin hepatocarcinogenicity by altering gene expression as a result of 8-OHdG adduct formation, but not by inducing DNA mutation. Therefore, consistent with a previous study by Tasaki et al. [15], it is reasonable to suggest that the hepatocarcinogenicity of Dammar resin observed in our previous long-term experiment with rats (unpublished data) may not be caused by DNA mutations, but rather by non-genotoxic mechanisms: Promotion of cell proliferation, induction of P450s, detoxification and antioxidant enzymes, increased intranuclear oxidative stress and other gene products. Although the mechanisms responsible for the carcinogenicity of Dammar resin remain to be further defined, our findings support the suggestion that its carcinogenicity does not necessarily correlate with in vivo mutagenicity [1].

In a recent study, 20 terpenoids from Dammar resin are pointed to have cytotoxic activity against human leukemia (HL60) and melanoma (RL1579) cells in vitro, which suggest that triterpenoids isolated from Dammar resin and its derivatives are valuable as potential cancer chemopreventive agents [7]. However, although no genetoxicity was observed in Dammar resin-treated group in the present study, considering its hepatocarcinogenesis in rats, Dammar resin should be used with care, if used at all, as a cancer chemopreventive agent until further investigations are conducted focusing on its metabolism and the underlying mechanisms of its hepatocarcinogenicity. Furthermore, the results of the present study suggest that Dammar resin has potential carcinogenic activity in mice.

In summay, administration of the known genotoxic hepatocarcinogen IQ results in increased liver cell proliferation and a characteristic mutation spectra with a predominant occurrence of G:C to T:A transitions in the *gpt* sequence analysis. Decreased expression of *cyp2e1* and *gpx1* increases the genotoxicity of IQ and decreased expression of p53 allows the survival and proliferation of cells with mutated DNA, suggesting that the hepatocarcinogenicity of IQ is initiated by DNA mutation. Like IQ, administration of Dammar resin to *gpt* delta mice also promotes liver cell proliferation; however, unlike IQ, Dammar resin administration does not cause DNA mutation. Rather, Dammar resin promotes cell proliferation, induces expression metabolic enzymes, and increases intranuclear oxidative stress. These results suggest that Dammar resin is a potential hepatocarcinogen in mice, although this remains to be verified. Dammar resin does not increase DNA mutation frequency, indicating that it is non-genotoxic in mice, which is consistent with our results of mutation assay conducted in *gpt* delta rats (manuscript in preparation). Importantly, the possible mechanism of Dammar resin-mediated carcinogenicity suggested by the results of the present study is also active in humans, indicating that the use of Dammar resin or its constituents in foods or as a food supplement for humans should be carefully monitored.

Conflict of interest statement

The authors declare that there are no conflicts of interest.

Acknowledgements

This work was partly supported by a Grant-in-Aid for Scientific Research from the Ministry of Health, Labor and Welfare of Japan. We thank Yumi Obo and Rie Onodera for their technical assistance and Yukiko Iura for her help during preparation of this manuscript.

References

[1] Y. Hayashi, Overview of genotoxic carcinogens and non-genotoxic carcinogens, Exp. Toxicol. Pathol. 44 (1992) 465–471.
[2] K. Wakabayashi, M. Nagao, H. Esumi, T. Sugimura, Food-derived mutagens and carcinogens, Cancer Res. 52 (1992) 2092s–2098s.
[3] K. Kanki, A. Nishikawa, K. Masumura, T. Umemura, T. Imazawa, Y. Kitamura, T. Nohmi, M. Hirose, In vivo mutational analysis of liver DNA in gpt delta transgenic rats treated with the hepatocarcinogens N-nitrosopyrrolidine, 2-amino-3-methylimidazo[4,5-*f*]quinoline, and di(2-ethylhexyl)phthalate, Mol. Carcinogen. 42 (2005) 9–17.
[4] H. Ohgaki, K. Kusama, N. Matsukura, K. Morino, H. Hasegawa, S. Sato, S. Takayama, T. Sugimura, Carcinogenicity in mice of a mutagenic compound, 2-amino-3-methylimidazo[4,5-*f*]quinoline, from broiled sardine, cooked beef and beef extract, Carcinogenesis 5 (1984) 921–924.
[5] S.A. Bol, J. Horlbeck, J. Markovic, J.G. de Boer, R.J. Turesky, A. Constable, Mutational analysis of the liver, colon and kidney of Big Blue rats treated with 2-amino-3-methylimidazo[4,5-*f*]quinoline, Carcinogenesis 21 (2000) 1–6.
[6] B.L. Poehland, B.K. Carte, T.A. Francis, L.J. Hyland, H.S. Allaudeen, N. Troupe, In vitro antiviral activity of dammar resin triterpenoids, J. Nat. Prod. 50 (1987) 706–713.
[7] M. Ukiya, T. Kikuchi, H. Tokuda, K. Tabata, Y. Kimura, T. Arai, Y. Ezaki, O. Oseto, T. Suzuki, T. Akihisa, Antitumor-promoting effects and cytotoxic activities of dammar resin triterpenoids and their derivatives, Chem. Biodivers. 7 (2010) 1871–1884.
[8] D. Kirkland, M. Aardema, L. Henderson, L. Muller, Evaluation of the ability of a battery of three in vitro genotoxicity tests to discriminate rodent carcinogens and non-carcinogens. I. Sensitivity, specificity and relative predictivity, Mutat. Res. 584 (2005) 1–256.
[9] A. Kinoshita, H. Wanibuchi, S. Imaoka, M. Ogawa, C. Masuda, K. Morimura, Y. Funae, S. Fukushima, Formation of 8-hydroxydeoxyguanosine and cell-cycle arrest in the rat liver via generation of oxidative stress by phenobarbital: association with expression profiles of p21(WAF1/Cip1), cyclin D1 and Ogg1, Carcinogenesis 23 (2002) 341–349.
[10] A. Sapone, B. Gustavino, M. Monfrinotti, D. Canistro, M. Broccoli, L. Pozzetti, A. Affatato, L. Valgimigli, G.C. Forti, G.F. Pedulli, G.L. Biagi, S.Z. Abdel-Rahman, M. Paolini, Perturbation of cytochrome P450, generation of oxidative stress and induction of DNA damage in Cyprinus carpio exposed in situ to potable surface water, Mutat. Res. 626 (2007) 143–154.
[11] K.D. Nichols, G.M. Kirby, Expression of cytochrome P450 2A5 in a glucose-6-phosphate dehydrogenase-deficient mouse model of oxidative stress, Biochem. Pharmacol. 75 (2008) 1230–1239.
[12] Y. Dewa, J. Nishimura, M. Muguruma, M. Jin, Y. Saegusa, T. Okamura, M. Tasaki, T. Umemura, K. Mitsumori, beta-Naphthoflavone enhances oxidative stress responses and the induction of preneoplastic lesions in a diethylnitrosamine-initiated hepatocarcinogenesis model in partially hepatectomized rats, Toxicology 244 (2008) 179–189.
[13] Y. Dewa, J. Nishimura, M. Muguruma, M. Jin, M. Kawai, Y. Saegusa, T. Okamura, T. Umemura, K. Mitsumori, Involvement of oxidative stress in hepatocellular tumor-promoting activity of oxfendazole in rats, Arch. Toxicol. 83 (2009) 503–511.
[14] M. Kawai, Y. Saegusa, Y. Dewa, J. Nishimura, S. Kemmochi, T. Harada, Y. Ishii, T. Umemura, M. Shibutani, K. Mitsumori, Elevation of cell proliferation via generation of reactive oxygen species by piperonyl butoxide contributes to its liver tumor-promoting effects in mice, Arch. Toxicol. 84 (2010) 155–164.
[15] M. Tasaki, T. Umemura, Y. Suzuki, D. Hibi, T. Inoue, T. Okamura, Y. Ishii, S. Maruyama, T. Nohmi, A. Nishikawa, Oxidative DNA damage and reporter gene mutation in the livers of gpt delta rats given non-genotoxic hepatocarcinogens with cytochrome P450-inducible potency, Cancer Sci. 101 (2010) 2525–2530.
[16] T. Nohmi, M. Katoh, H. Suzuki, M. Matsui, M. Yamada, M. Watanabe, M. Suzuki, N. Horiya, O. Ueda, T. Shibuya, H. Ikeda, T. Sofuni, A new transgenic mouse mutagenesis test system using Spi- and 6-thioguanine selections, Environ. Mol. Mutagen. 28 (1996) 465–470.
[17] K. Masumura, M. Matsui, M. Katoh, N. Horiya, O. Ueda, H. Tanabe, M. Yamada, H. Suzuki, T. Sofuni, T. Nohmi, Spectra of gpt mutations in ethylnitrosourea-treated and untreated transgenic mice, Environ. Mol. Mutagen. 34 (1999) 1–8.
[18] K. Masumura, Y. Totsuka, K. Wakabayashi, T. Nohmi, Potent genotoxicity of aminophenylnorharman, formed from non-mutagenic norharman and aniline, in the liver of gpt delta transgenic mouse, Carcinogenesis 24 (2003) 1985–1993.
[19] T. Suzuki, M. Hayashi, M. Ochiai, K. Wakabayashi, T. Ushijima, T. Sugimura, M. Nagao, T. Sofuni, Organ variation in the mutagenicity of MeIQ in Big Blue lacI transgenic mice, Mutat. Res. 369 (1996) 45–49.
[20] J.A. Heddle, P. Shaver-Walker, K.S. Tao, X.B. Zhang, Treatment protocols for transgenic mutation assays in vivo, Mutagenesis 10 (1995) 467–470.
[21] T. Suzuki, S. Itoh, M. Nakajima, N. Hachiya, T. Hara, Target organ and time-course in the mutagenicity of five carcinogens in MutaMouse: a summary report of the second collaborative study of the transgenic mouse mutation assay by JEMS/MMS, Mutat. Res. 444 (1999) 259–268.
[22] M. Wei, H. Wanibuchi, D. Nakae, H. Tsuda, S. Takahashi, M. Hirose, Y. Totsuka, M. Tatematsu, S. Fukushima, Low-dose carcinogenicity of 2-amino-3-methylimidazo[4,5-*f*]quinoline in rats: evidence for the existence of no-effect levels and a mechanism involving p21(Cip/WAF1), Cancer Sci. 102 (2011) 88–94.
[23] V.M. Lakshmi, F.F. Hsu, T.V. Zenser, N-Demethylation is a major route of 2-amino-3-methylimidazo[4,5-*f*]quinoline metabolism in mouse, Drug Metab. Dispos. 36 (2008) 1143–1152.
[24] J. Gerdes, U. Schwab, H. Lemke, H. Stein, Production of a mouse monoclonal antibody reactive with a human nuclear antigen associated with cell proliferation, Int. J. Cancer 31 (1983) 13–20.
[25] M. Nolte, M. Werner, A. Nasarek, H. Bektas, R. von Wasielewski, J. Klempnauer, A. Georgii, Expression of proliferation associated antigens and detection of numerical chromosome aberrations in primary human liver tumours: relevance to tumour characteristics and prognosis, J. Clin. Pathol. 51 (1998) 47–51.
[26] Y. Kitamura, T. Umemura, K. Okazaki, K. Kanki, T. Imazawa, T. Masegi, A. Nishikawa, M. Hirose, Enhancing effects of simultaneous treatment with sodium nitrite on 2-amino-3-methylimidazo[4,5-*f*]quinoline-induced rat liver, colon and Zymbal's gland carcinogenesis after initiation with diethylnitrosamine and 1,2-dimethylhydrazine, Int. J. Cancer 118 (2006) 2399–2404.
[27] J.E. Klaunig, Y. Xu, J.S. Isenberg, S. Bachowski, K.L. Kolaja, J. Jiang, D.E. Stevenson, E.F. Walborg Jr., The role of oxidative stress in chemical carcinogenesis, Environ. Health Perspect. 106 (Suppl. 1) (1998) 289–295.
[28] S.W. Lowe, A.W. Lin, Apoptosis in cancer, Carcinogenesis 21 (2000) 485–495.
[29] C.A. Schmitt, J.S. Fridman, M. Yang, E. Baranov, R.M. Hoffman, S.W. Lowe, Dissecting p53 tumor suppressor functions in vivo, Cancer Cell 1 (2002) 289–298.
[30] Z.N. Oltvai, C.L. Milliman, S.J. Korsmeyer, Bcl-2 heterodimerizes in vivo with a conserved homolog, Bax, that accelerates programmed cell death, Cell 74 (1993) 609–619.
[31] L. Buckbinder, R. Talbott, S. Velasco-Miguel, I. Takenaka, B. Faha, B.R. Seizinger, N. Kley, Induction of the growth inhibitor IGF-binding protein 3 by p53, Nature 377 (1995) 646–649.
[32] T. Miyashita, J.C. Reed, Tumor suppressor p53 is a direct transcriptional activator of the human bax gene, Cell 80 (1995) 293–299.
[33] A. Thomas, T. Giesler, E. White, p53 mediates bcl-2 phosphorylation and apoptosis via activation of the Cdc42/JNK1 pathway, Oncogene 19 (2000) 5259–5269.
[34] M.T. Hemann, S.W. Lowe, The p53-Bcl-2 connection, Cell Death Differ. 13 (2006) 1256–1259.
[35] S. Kothakota, T. Azuma, C. Reinhard, A. Klippel, J. Tang, K. Chu, T.J. McGarry, M.W. Kirschner, K. Koths, D.J. Kwiatkowski, L.T. Williams, Caspase-3-generated fragment of gelsolin: effector of morphological change in apoptosis, Science 278 (1997) 294–298.
[36] S. Ghavami, M. Hashemi, S.R. Ande, B. Yeganeh, W. Xiao, M. Eshraghi, C.J. Bus, K. Kadkhoda, E. Wiechec, A.J. Halayko, M. Los, Apoptosis and cancer: mutations within caspase genes, J. Med. Genet. 46 (2009) 497–510.
[37] A.H. Conney, Induction of microsomal enzymes by foreign chemicals and carcinogenesis by polycyclic aromatic hydrocarbons: G.H.A. Clowes Memorial Lecture, Cancer Res. 42 (1982) 4875–4917.
[38] X. Chen, T.O. Scholl, M.J. Leskiw, M.R. Donaldson, T.P. Stein, Association of glutathione peroxidase activity with insulin resistance and dietary fat intake during normal pregnancy, J. Clin. Endocrinol. Metab. 88 (2003) 5963–5968.
[39] J.D. Hayes, D.J. Pulford, The glutathione S-transferase supergene family: regulation of GST and the contribution of the isoenzymes to cancer chemoprotection and drug resistance, Crit. Rev. Biochem. Mol. Biol. 30 (1995) 445–600.
[40] R.A. McPherson, M.D. Tingle, L.R. Ferguson, Contrasting effects of acute and chronic dietary exposure to 2-amino-3-methyl-imidazo[4,5-*f*]quinoline (IQ) on xenobiotic metabolising enzymes in the male Fischer 344 rat: implications for chemoprevention studies, Eur. J. Nutr. 40 (2001) 39–47.
[41] E.T. Morgan, K.B. Goralski, M. Piquette-Miller, K.W. Renton, G.R. Robertson, M.R. Chaluvadi, K.A. Charles, S.J. Clarke, M. Kacevska, C. Liddle, T.A. Richardson, R. Sharma, C.J. Sinal, Regulation of drug-metabolizing enzymes and transporters in infection, inflammation, and cancer, Drug Metab. Dispos. 36 (2008) 205–216.
[42] K. Shimamoto, Y. Dewa, Y. Ishii, S. Kemmochi, E. Taniai, H. Hayashi, M. Imaoka, R. Morita, K. Kuwata, K. Suzuki, M. Shibutani, K. Mitsumori, Indole-3-carbinol enhances oxidative stress responses resulting in the induction of preneoplastic liver cell lesions in partially hepatectomized rats initiated with diethylnitrosamine, Toxicology 283 (2011) 109–117.
[43] Y. Minamiyama, S. Takemura, S. Toyokuni, S. Imaoka, Y. Funae, K. Hirohashi, T. Yoshikawa, S. Okada, CYP3A induction aggravates endotoxemic liver injury via reactive oxygen species in male rats, Free Radic. Biol. Med. 37 (2004) 703–712.

J Toxicol Pathol 2013; 26: 335–341

Review

Colon Preneoplastic Lesions in Animal Models

Masumi Suzui[1*], Takamitsu Morioka[2], and Naoki Yoshimi[3]

[1] Department of Molecular Toxicology, Graduate School of Medical Sciences and Medical School, Nagoya City University, 1 Kawasumi, Mizuho-ku, Mizuho-cho, Nagoya 467-8601, Japan
[2] Radiation Effect Accumulation and Prevention Project, Fukushima Project Headquarters and Radiobiology for Children's Health Program, Research Center for Radiation Protection, National Institute of Radiological Sciences, 4-9-1 Anagawa, Inage-ku, Chiba 263-8555, Japan
[3] Department of Pathology and Oncology, Graduate School of Medicine and Faculty of Medicine, University of the Ryukyus Faculty of Medicine, 207 Uehara, Nishihara-cho, Okinawa 903-0215, Japan

Abstract: The animal model is a powerful and fundamental tool in the field of biochemical research including toxicology, carcinogenesis, cancer therapeutics and prevention. In the carcinogenesis animal model system, numerous examples of preneoplastic lesions have been isolated and investigated from various perspectives. This may indicate that several options of endpoints to evaluate carcinogenesis effect or therapeutic outcome are presently available; however, classification of preneoplastic lesions has become complicated. For instance, these lesions include aberrant crypt foci (ACF), dysplastic ACF, flat ACF, β-catenin accumulated crypts, and mucin-depleted foci. These lesions have been induced by commonly used chemical carcinogens such as azoxymethane (AOM), 1,2-dimethylhydrazine (DMH), methylnitrosourea (MUN), or 2-amino-1-methyl-6-phenylimidazo[4,5-*b*]pyridine (PhIP). Investigators can choose any procedures or methods to examine colonic preneoplastic lesions according to their interests and the objectives of their experiments. Based on topographical, histopathological, and biological features of colon cancer preneoplastic lesions in the animal model, we summarize and discuss the character and implications of these lesions. (DOI: 10.1293/tox.2013-0028; J Toxicol Pathol 2013; 26: 335–341)

Key words: preneoplastic lesion, colon carcinogenesis, animal model, topographic view

Aberrant Crypt Foci (ACF)

Bird[1] first reported in 1987 that when C57BL/6J mice were treated with azoxymethane (AOM), aberrant dysplastic crypts appeared in the colonic mucosa. After fixation with 10% buffered formalin and staining with methylene blue, these crypts were easily visualized in the topographic view of the colonic mucosa using a x4 objective (Fig. 1A). These lesions were referred to as aberrant crypts (AC) or aberrant crypt foci (ACF) in the colon of both animals and humans[2–4]. ACF were cryptic lesions distinguished by their increased size, thicker epithelial lining, and increased pericryptic zone[1]. ACF have only been seen in the colon of carcinogen-treated mice and rats. They have not been seen in the colon treated with a noncarcinogen or in untreated animals[2,3]. After carcinogen treatment, they appeared as early as within 2 weeks and persisted until the experimental termination of animals (16 weeks); histological changes from mild atypia to dysplasia[2] were also revealed. Two heterocyclic amines, 2-amino-3-methylimidazo[4,5-*f*]quinoline (IQ) and 2-amino-1-methyl-6-phenylimidazo[4,5-*b*]pyridine (PhIP), were shown to be able to induce ACF in the colon, respectively, after 4 and 10 weeks of exposure[5]. The number of ACF increased significantly over time, and small-sized ACF were predominant at all time points[5]. In histological slides, the large ACF exhibits dysplasia and thus can be termed a microadenoma[2].

ACF are also induced in the colonic mucosa of rats or mice treated with carcinogens such as AOM, methylazoxymethanol (MAM) acetate, 1,2-dimethylhydrazine (DMH), methylnitrosourea (MNU), PhIP, IQ, 2-amino-3,8-dimethylimidazo[4,5-*f*]quinoline (MeIQ) and 2-amino-6-methyldipyrido[1,2-*a*:3',2'-*d*]imidazole (Glu-P-1)[3,6–11]. In our previous experiments[7,12], F344 rats were subcutaneously (sc) injected with AOM (20 mg/kg body weight) twice. Five weeks after the beginning of the experiment, 93–139 ACF per colon occurred. When F344 rats were treated with AOM (15 mg/kg body weight, sc injection) 3 times, 240 ACF/colon occurred at 11 weeks after the beginning of the experiment[13]. When F344 rats were treated with DMH (40 mg/kg body weight, sc injection) twice, 175–200 ACF/colon were induced at 5 or 8 weeks after the beginning of the experiment[11,14,15]. These ACF usually contained 1–3 or more crypts per focus. The diameter of an aberrant crypt measured at least 3 to 4 times larger than that of a normal crypt

Received: 28 May 2013, Accepted: 27 June 2013
*Corresponding author: M Suzui (suzui@med.nagoya-cu.ac.jp)
©2013 The Japanese Society of Toxicologic Pathology
This is an open-access article distributed under the terms of the Creative Commons Attribution Non-Commercial No Derivatives (by-nc-nd) License <http://creativecommons.org/licenses/by-nc-nd/3.0/>.

in mice[2,16] and up to 1.5 times larger than a normal crypt in humans[17]. Pretlow *et al.*[16] reported that ACF were at least 3 times larger in diameter than normal crypts, and most ACF had lumina that were oval or slit shaped rather than circular. ACF range in size and have from 1 to 412 aberrant crypts per focus[17–20]. The size in the topographic view and the histologically dysplastic character of ACF are critical factors when we distinguish ACF as preneoplastic lesions. We consider that large ACF consisting of more than 10–20 crypts and manifesting dysplasia could be termed a microadenoma. In mouse models, for instance, B57BL/6J and CF_1 mice were given a single intraperitoneal (ip) injection of AOM (5 mg/kg body weight), and 4 weeks later, mice developed 2.6 and 3 ACF per colon, respectively[2]. BALB/c mice were ip injected with AOM (10 mg/kg body weight) twice, and 14 ACF were induced 4 weeks after the injection[21]. In C57BL/6J-*Min*/+ (*Min*) and C57BL/6J-+/+ (wild type) mice, PhIP was ip injected 4 times. Ten weeks after the injection, male mice developed 3 and 0 ACF, respectively, and female mice developed 1.9 and 0.2 ACF in their colons[22]. These findings indicate that duration of the experimental period, strain of animals, method of administration of carcinogens, and nature of carcinogen used as an initiator, may affect the number of ACF in the colonic mucosa.

In terms of the distribution of ACF, McLellan *et al.*[2] demonstrated that AOM-treated CF_1 mice developed ACF, 67% of which were in the rectal segment, 29% of which were in the middle segment and 4% of which were in the cecal segment. ACF were seen mainly in the rectal and middle segments when the animals were treated with DMH, NMU, MeIQ, or Glu-P-1[3]. Most ACF were found in the middle and distal colon in F344 rats treated with AOM[23]. In contrast, Hata *et al.*[24] demonstrated that ACF were frequently found in the proximal colon (cecal segment of the colon) when AKR/J and SWR/J mice were treated with AOM. The carcinogen IQ also induced ACF primarily in the middle and cecal segments of the colon[3]. Colon tumors induced by AOM were primarily found in distal colon rather than in proximal colon in the rat and mouse models[24,25], indicating that the correlation between ACF formation and carcinogenesis is not necessarily straightforward. This is presumably because of the heterogeneous nature of ACF[26–28]. Also, experimental protocol and species used may affect the difference in distribution of ACF[3,29–31].

The shape of the lumen of the ACF is relates to the histology of the ACF. Histological criteria of rat/mouse ACF have been described by several investigators[26,32]. Accordingly, ACF may be classified into the following 3 categories. In brief, these are (1) non dysplastic foci, which exhibit hypercellularity of uniform or normal looking goblet cells with basal-oriented nuclei and apical localization of mucus; (2) mild to moderate dysplastic foci, which exhibit hypercellularity of cells with elongated nuclei and focal nuclear stratification; and (3) moderate to severe dysplastic foci, which exhibit hypercellularity of elongated cells with abundant basophilic cytoplasm. These foci display enlarged and vesiculated nuclei, sometimes with prominent nucleoli.

Dysplastic ACF

The dysplastic nature of ACF was described by McLellan and Bird[2]. In a hematoxylin-eosin (HE) stained transverse section, ACF exhibited a focal appearance and mild cellular atypia, and dysplasia was observed in the large focus. Bird and Pretlow mentioned that use of the term dysplastic crypt foci to describe abnormal crypts is valid only if the investigators examined histologically all of the methylene blue-identified lesions and found dysplasia in all of them[33]. Ochiai *et al.*[34,35] described two distinct types of ACF in the PhIP-induced rat model. One was dysplastic ACF, and the other was nondysplastic ACF. In their reports, dysplastic ACF are histologically characterized by distortion of the crypt structure, a decrease in goblet cell number, existence of nuclear stratification, and enlarged nuclei. Nondysplastic ACF indicated the hyperplastic change in crypts. One-fourth of PhIP-induced ACF were dysplastic ACF, and the remaining ACF were nondysplastic ACF. Two-week dietary administration of 400 ppm PhIP was repeated three times with a 4-week interval. The average number of dysplastic ACF was up to 0.8 per colon, and they were larger in size than nondysplastic ACF after 32 weeks of experimentation. In the dysplastic ACF, cytoplasmic β-catenin protein accumulation and β-catenin gene mutation were found. The mutations were $^{32}A \rightarrow G$ (Asp→Gly), $^{34}G \rightarrow T$ (Gly→Val), and $^{36}C \rightarrow T$ (His→Tyr)[35]. By a staining method that uses 70% methanol followed by 0.2% methylene blue staining, dysplastic ACF can be topographically contrasted with nondysplastic ACF on the colonic mucosa and identified without performing histological examination[34]. The average number of dysplastic ACF/colon was 2.0–3.2 in F344 rats treated with PhIP (400 ppm in diet), MeIQ (300 ppm in diet), and IQ (300 ppm in diet). Two-week dietary administration of PhIP, MeIQ, or IQ was repeated three times with a 4-week interval. Other investigators[26,32,34,36] have also described dysplastic ACF. Thorup[32] found that a correlation between degree of dysplasia and crypt multiplicity, indicating that chemically induced ACF can increase in crypt multiplicity over time and progress into a tumor and that hyperplastic human ACF can also develop into adenomatous ACF, as reported elsewhere[37,38]. However, this view disagrees with that of other studies[39–41] demonstrating that the degree of dysplasia is not necessarily related to the crypt multiplicity.

Flat ACF

Paulsen *et al.*[42] examined unsectioned methylene blue-stained colon tissues obtained from male F344 rats treated with AOM (sc injection ×2 times, 15 mg/kg body weight), and found two types of early lesions. One was classic elevated ACF, and the other was flat ACF. Classical ACF were seen as enlarged crypts that were elevated from the surrounding epithelium and had elongated luminal openings. However, Paulsen *et al.*[42] described flat ACF as structures that were not elevated. The bright blue appearance and compressed pit pattern of flat ACF were used as criteria for identification.

Flat ACF were characterized by enlarged or small crypts that were not elevated from the epithelium and had round or elongated luminal openings. The investigators also described histological findings of flat ACF with severe dysplasia. In immunohistochemical analysis, classic elevated ACF did not show (0 of 99) cytoplasmic/nuclear expression of the β-catenin protein. In contrast, all flat ACF (8 of 8) displayed cytoplasmic/nuclear expression of the β-catenin protein. The number of classic elevated ACF decreased along with time. Their crypt multiplicity increased during the time period. The number of flat ACF decreased along time, and that of tumors increased correspondingly. The numbers of flat ACF plus tumors were virtually constant. In view of these findings, Paulsen *et al.*[42] concluded that flat ACF display a continuous development from early stages into a tumor.

β-Catenin Accumulated Crypts (BCAC)

In a previous study, we[43] found that focal lesions that display accumulation of the β-catenin protein predispose to carcinogen-induced colon carcinogenesis. We named these lesions β-catenin-accumulated crypts (BCAC) (Fig. 1B). F344 rats were treated with AOM (sc injection ×3 times, 15 mg/kg body weight), and a complete autopsy was performed at 10 weeks after the first AOM treatment[43]. In the topographical view in which colon tissues were stained with methylene blue, we found distinct populations of altered crypts named histologically altered crypts with macroscopically normal-like appearance (HACN) among the tissue samples. In HACN, which are equivalent to BCAC, the *β-catenin* gene was frequently mutated in 10 of 15 samples (67%), and the cytoplasmic β-catenin protein was accumulated in 13 of 15 samples (86%)[43]. Among these lesions, there were ^{28}A→T (Gln→His), ^{29}C→G (Ser→Cys), ^{30}T→C (Tyr→His), ^{32}G→A (Asp→Asn), ^{34}G→A (Gky→Glu), ^{34}G→T (Gly→stop), and ^{41}A→T (Thr→Ile) mutations. Because the lesion in which the β-catenin protein accumulated was considered to be valid in AOM-treated rat colonic mucosa, a time course study was done to examine the status of the protein accumulation, the number of crypts/lesion, and the diameter of the crypts[44]. Both the number of crypts/lesion and the diameter of the β-catenin accumulated crypts that were identified with immunohistochemical analysis significantly increased with the time course[24]. The number of BCAC induced by AOM in AKR/J and SWR/J mice varied by 3–12 per cm^2, and multiplicity was about 3–4 in both strains[24]. Histological abnormality of the crypts and cell proliferation also significantly increased when compared with those of ACF, indicating that BCAC are preneoplastic lesions in AOM-induced colon carcinogenesis[44].

Mucin-depleted Foci (MDF)

Caderni *et al.*[45] identified specific lesions in the colon of rats treated with AOM. When unsectioned colon tissues were stained with high-iron diamine-Alcian blue (HID-AB), foci of crypts with scarce or absent mucins were seen, and such lesions were first defined as mucin-depleted foci (MDF) (Fig. 1C). In that study, male F344 rats received sc injection of AOM (15 mg/kg body weight) twice. The rats developed approximately 4 and 8 MDF/colon at 7 and 15 weeks, respectively, after the start of the experiment, while 271–289 ACF/colon occurred during the same period. Mutations in *β-catenin*, *Apc*, and *K-ras* genes and cytoplasmic β-catenin expression were found in MDF induced by DMH[46–48]. Among these, *β-catenin* gene mutations included ^{32}G→A (Asp→Asn), ^{37}C→T (Ser→Phe), ^{33}C→T (Ser→Phe), and ^{41}C→T (Thr→Ile). In DMH studies, MDF exhibit dysplastic features, and the induction rate of MDF is dose dependent[45,47]. Also, MDF increase in size with time. To examine the multiplicity and distribution of ACF, MDF, and tumors, six-week-old F344 rats were treated with DMH (40 mg/kg body weight sc injection twice a week) followed by 1% dextran sodium sulfate in drinking water. At ten and fourteen weeks after the start of the experiment, animals were euthanized. ACF were mainly found in the middle portion of the colon (Fig. 2A). MDF and tumors occurred more in the distal portion than in the proximal portion (Fig. 2B and C). These results were in accordance with those in the report of Femia *et al*[47]. They found that DMH-induced MDF and tumors were mainly found in the distal portion of the colon, while "classical" ACF were found more predominantly in the middle portion of the colon[47]. Also, Femia *et al.* mentioned that with regard to the ability of ACF/MDF as a biomarker predicting the carcinogenesis status, the heterogeneous nature of each lesion may be related[49].

Only a limited number of findings on MDF are currently available; based on those that are available, Femia and Caderny[27] conclude that MDF are premalignant lesions for colon carcinogenesis and a promising biomarker for study of the effect of chemopreventive agents in colon carcinogenesis. MDF may provide a reliable option as biomarkers for colon carcinogenesis, and it is thought that production or deletion of mucin or both plays some roles in the development of colon tumors. To reiterate, MDF may have both morphological and biochemical aspects as a biomarker. To identify MDF, we[11] demonstrated a simple staining method using 1% Alcian blue (pH 2.5) solution instead of the original HID-AB staining method. In this study, male F344 received sc injections of DMH (40 mg/kg body weight) twice, and the rats developed 19 MDF/colon and 150 ACF/colon at 8 weeks after the start of the experiment. By comparing exact locations of MDF and BCAC on the face-up mucosal samples and by conducting Alcian blue/HE/immunohistochemical staining, we[11] found that MDF are practically identical to BCAC and useful as an early biomarker in rat colon carcinogenesis. In human specimens obtained from patients with colorectal carcinoma (CRC) and familial adenomatous polyposis (FAP), MDF were also identified[50]. The mean numbers of crypts/MDF were 60 and 33 in samples of patients with CRC and FAP, respectively. In a CRC case, the histological diagnosis of MDF was microadenoma with moderate grade dysplasia, while in cases of FAP, the diagnosis was microadenoma with low-grade dysplasia[50]. In a recent

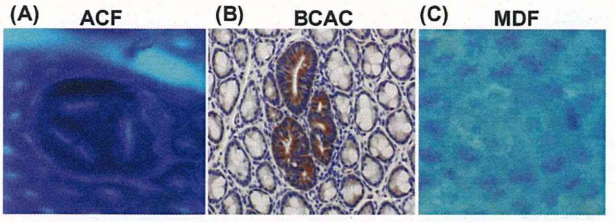

Fig. 1. Topographic views of (A) ACF, (B) BCAC, and (C) MDF. (A) Note that three identical crypts are seen in one focus (methylene blue staining). (B) Crypts with accumulations of β-catenin protein in cytoplasm are present (immunohistochemical staining). (C) A focal lesion characterized by the absence or very small production of mucin (seen as very thin blue-stained crypts) is present (high-iron diamine-Alcian blue staining). ACF, aberrant crypt foci; BCAC, β-catenin accumulated crypts; MDF, mucin-depleted foci.

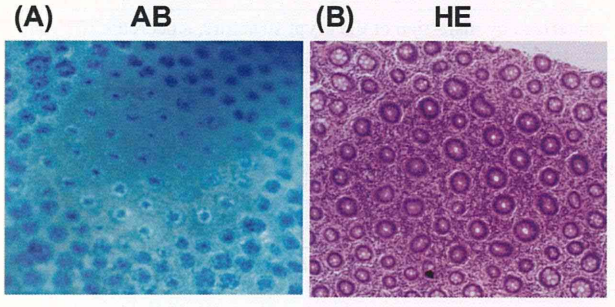

Fig. 3. Topographic views of human MDF stained with (A) 1% Alcian blue (pH 2.5) and (B) hematoxylin and eosin. MDF were identified as focal lesions characterized by loss of Alcian blue staining, attributable to the loss of mucin, as compared with the surrounding normal crypts. AB, Alcian blue; HE, hematoxylin and eosin.

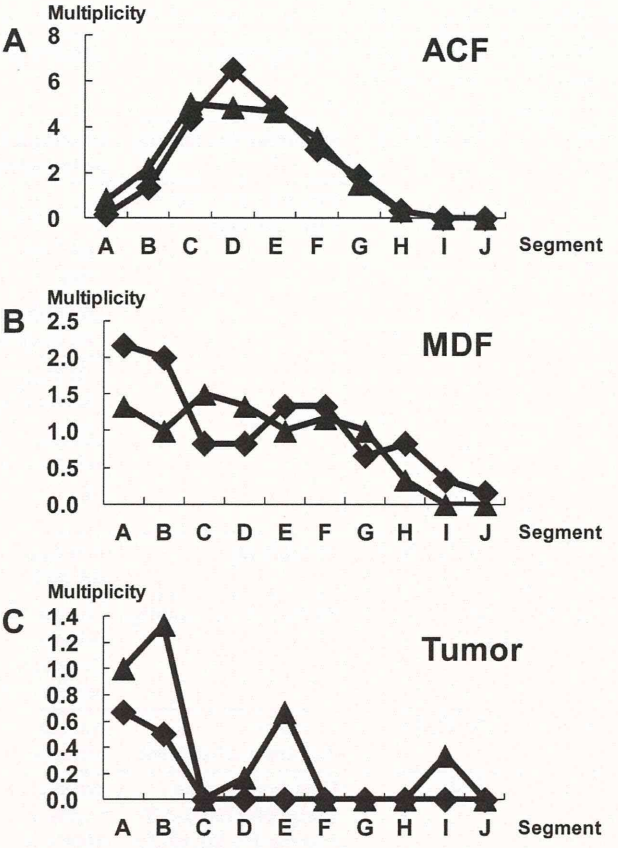

Fig. 2. Distribution of ACF, MDF, and tumors in each segment (A-J) along the colon. The x-axis indicates the segments from the distal to proximal colon. Each segment was named A to J in 2-cm intervals from the anal side. The y-axis indicates the average number of lesions per colon (multiplicity). At ten (closed diamond) and fourteen weeks (closed triangle) after the start of the experiment, animals were euthanized. After fixing of colon tissues with 10% buffered formalin on a filter paper with the mucosal surface up, colon tissues were stained with a 1% solution of Alcian blue, pH 2.5, in 3% acetic acid for 5 min and immediately washed with distilled water. Subsequently, after detection of MDF, the colon tissue was stained with 0.2% methylene blue solution to identify ACF. ACF, MDF, and tumors were noted grossly for their location, number, and size as described earlier[11]. The animal experiment was conducted according to the Institutional Animal Care Guidelines.

study, our group[51] examined human CRC cases and found MDF on the colonic mucosa. The lesion was histologically classified into two categories: flat MDF and protruded MDF. The former lesion did not show nuclear stratification or loss of polarity, but showed Paneth cell metaplasia and decrease/loss of goblet cells, indicative of low-grade dysplasia. Protruded MDF displayed the features of both ACF and MDF, also corresponding to low-grade dysplasia. A topographic view of human MDF is shown in Fig. 3.

Conclusions

This review summarizes topographical, histopathological, and biological features of preneoplastic lesions that have been described in colon carcinogenesis models of the rodent (Table 1). The early lesion has been identified and documented as a preneoplastic lesion in the carcinogenesis process. However, the fact that even the verified lesions appear to contain neoplastic lesions such as a microadenoma indicates the need for further investigation. This may be due to complicated categories or classifications of preneoplastic lesions. Considering the 3R principles (which commonly consist of replacement of methods with no animal use, reduction of the number of test animals, and refinement of methods that minimize the suffering of test animals), a short-term experiment in which an early preneoplastic lesion occurs and can be used as a biomarker should be used to examine toxicity and/or carcinogenicity of test compounds in a specific organ site. In this context, investigators can choose any procedures or methods to examine colonic preneoplastic lesions according to their interests and the objectives of their experiments.

Table 1. Summary of Characters of Preneoplastic Lesions in the Animal Model

Practical name of the lesion	Ref. no. of the current article	Staining method	Features in topographic and/or histological views	
ACF	1, 2, 11, 26, 32	Methelene blue staining	In topographic view, increased cryptial size, thicker epilbelial linig, and increased pericryptical zone.	
		Hematoxylin-eosin (HE) staining	Histological criteria of ACF	
			(1) Non dysplastic foci	Hyercellularity of uniform or normal looking goblet cells with basal-oriented nuclei and apical localization of mucus.
			(2) Mild to moderate dysplastic foci	Hypercellularity of cells with elongated nuclei and focal nuclear stratification.
			(3) Moderate to severe dysplastic foci	Hypercellularity of elongated cells with abundant basophilic cytoplasm. These foci display enlarged and vesiculated nuclei, sometimes with prominent nucleoli.
			Subtype: dysplastic foci	Focal lesions with nuclear stratification, loss of nuclear polarity, structural abnormality of the crypts, Paneth cell metaplasia, a decrease or loss of goblet cells, and presence of mitosis.
Dysplastic ACF	26, 32, 34–36	HE staining	Histologically characterized by distortion of the crypt structure, a decrease in goblet cell number, nuclear stratification, and enlarged nuclei.	
Flat ACF	42	Methelene blue staining	Characterized by bright blue staining, enlarged or small crypts not elevated from the epithelium and round or elongated luminal openings. Because the flat ACF were not observed as elevated structures, their bright blue appearance and compressed pit pattern were used for identification.	
BCAC	24, 43, 44	Immuno-histochemical staining	Accumulation of cytoplasmic β-catenin protein. Crypts of BCAC do not display prominent epithelial cells in a topographic view.	
MDF	11, 45–50	High-iron diamine Alcian blue (HID-AB) staining 1% AB, pH2.5	When colon tissues were stained with HID-AB, foci of crypts with scarce or absent mucin were defined as MDF. MDF can be stained with 1% AB solution.	

ACF, aberrant crypt foci; BCAC, β-catenin accumulated crypts; MDF, mucin-depleted foci.

Acknowledgment: We thank Dr. Tatsuya Kinjo (Department of Digestive and General Surgery, University of the Ryukyus Graduate School of Medicine and Faculty of Medicine, Okinawa, Japan) for valuable comments and discussions. This work was supported in part by a Grant-in-Aid from the Ministry of Education, Culture, Sports, Science and Technology of Japan and a Grant-in-Aid from the Ministry of Health, Labour and Welfare.

References

1. Bird RP. Observation and quantification of aberrant crypts in the murine colon treated with a colon carcinogen: preliminary findings. Cancer Lett. **37**: 147–151. 1987. [Medline]
2. McLellan EA, and Bird RP. Aberrant crypts: potential preneoplastic lesions in the murine colon. Cancer Res. **48**: 6187–6192. 1988. [Medline]
3. Tudek B, Bird RP, and Bruce WR. Foci of aberrant crypts in the colons of mice and rats exposed to carcinogens associated with foods. Cancer Res. **49**: 1236–1240. 1989. [Medline]
4. Roncucci L, Stamp D, Medline A, Cullen JB, and Bruce WR. Identification and quantification of aberrant crypt foci and microadenomas in the human colon. Hum Pathol. **22**: 287–294. 1991. [Medline]
5. Kristiansen E. The role of aberrant crypt foci induced by the two heterocyclic amines 2-amino-3-methyl-imidazo[4,5-*f*]quinoline (IQ) and 2-amino-1-methyl-6-phenyl-imidazo[4,5-*b*]pyridine (PhIP) in the development of colon cancer in mice. Cancer Lett. **110**: 187–192. 1996. [Medline]
6. Bird RP. Role of aberrant crypt foci in understanding the pathogenesis of colon cancer. Cancer Lett. **93**: 55–71. 1995. [Medline]
7. Morioka T, Suzui M, Nabandith V, Inamine M, Aniya Y, Nakayama T, Ichiba T, Mori H, and Yoshimi N. The modifying effect of *Peucedanum japonicum*, a herb in the Ryukyu Islands, on azoxymethane-induced colon preneoplastic lesions in male F344 rats. Cancer Lett. **205**: 133–141. 2004. [Medline]
8. Mori Y, Yoshimi N, Iwata H, Tanaka T, and Mori H. The synergistic effect of 1-hydroxyanthraquinone on methylazoxymethanol acetate-induced carcinogenesis in rats. Carcinogenesis. **12**: 335–338. 1991. [Medline]
9. Chewonarin T, Kinouchi T, Kataoka K, Arimochi H, Kuwahara T, Vinitketkumnuen U, and Ohnishi Y. Effects of roselle (Hibiscus sabdariffa Linn.), a Thai medicinal plant, on the mutagenicity of various known mutagens in Salmonella typhimurium and on formation of aberrant crypt foci induced by the colon carcinogens azoxymethane and 2-amino-1-methyl-6-phenylimidazo[4,5-*b*]pyridine in F344 rats. Food Chem Toxicol. **37**: 591–601. 1999. [Medline]
10. Sohn OS, Fiala ES, Requeijo SP, Weisburger JH, and Gonzalez FJ. Differential effects of CYP2E1 status on the meta-

bolic activation of the colon carcinogens azoxymethane and methylazoxymethanol. Cancer Res. **61**: 8435–8440. 2001. [Medline]

11. Yoshimi N, Morioka T, Kinjo T, Inamine M, Kaneshiro T, Shimizu T, Suzui M, Yamada Y, and Mori H. Histological and immunohistochemical observations of mucin-depleted foci (MDF) stained with Alcian blue, in rat colon carcinogenesis induced with 1,2-dimethylhydrazine dihydrochloride. Cancer Sci. **95**: 792–797. 2004. [Medline]
12. Morioka T, Suzui M, Nabandith V, Inamine M, Aniya Y, Nakayama T, Chiba T, and Yoshimi N. Modifying effects of Terminalia catappa on azoxymethane-induced colon carcinogenesis in male F344 rats. Eur J Cancer Prev. **14**: 101–105. 2005. [Medline]
13. Asano N, Kuno T, Hirose Y, Yamada Y, Yoshida K, Tomita H, Nakamura Y, and Mori H. Preventive effects of a flavonoid myricitrin on the formation of azoxymethane-induced premalignant lesions in colons of rats. Asian Pac J Cancer Prev. **8**: 73–76. 2007. [Medline]
14. Nabandith V, Suzui M, Morioka T, Kaneshiro T, Kinjo T, Matsumoto K, Akao Y, Iinuma M, and Yoshimi N. Inhibitory effects of crude α-mangostin, a xanthone derivative, on two different categories of colon preneoplastic lesions induced by 1, 2-dimethylhydrazine in the rat. Asian Pac J Cancer Prev. **5**: 433–438. 2004. [Medline]
15. Inamine M, Suzui M, Morioka T, Kinjo T, Kaneshiro T, Sugishita T, Okada T, and Yoshimi N. Inhibitory effect of dietary monoglucosylceramide 1-O-β-glucosyl-*N*-2'-hydroxyarachidoyl-4,8-sphingadienine on two different categories of colon preneoplastic lesions induced by 1,2-dimethylhydrazine in F344 rats. Cancer Sci. **96**: 876–881. 2005. [Medline]
16. Pretlow TP, Barrow BJ, Ashton WS, O'Riordan MA, Pretlow TG, Jurcisek JA, and Stellato TA. Aberrant crypts: putative preneoplastic foci in human colonic mucosa. Cancer Res. **51**: 1564–1567. 1991. [Medline]
17. Fenoglio-Preiser CM, and Noffsinger A. Aberrant crypt foci: A review. Toxicol Pathol. **27**: 632–642. 1999. [Medline]
18. Di Gregorio C, Losi L, Fante R, Modica S, Ghidoni M, Pedroni M, Tamassia MG, Gafà L, Ponz de Leon M, and Roncucci L. Histology of aberrant crypt foci in the human colon. Histopathology. **30**: 328–334. 1997. [Medline]
19. Nucci MR, Robinson CR, Longo P, Campbell P, and Hamilton SR. Phenotypic and genotypic characteristics of aberrant crypt foci in human colorectal mucosa. Hum Pathol. **28**: 1396–1407. 1997. [Medline]
20. Shpitz B, Bomstein Y, Mekori Y, Cohen R, Kaufman Z, Neufeld D, Galkin M, and Bernheim J. Aberrant crypt foci in human colons: distribution and histomorphologic characteristics. Hum Pathol. **29**: 469–475. 1998. [Medline]
21. Osawa E, Nakajima A, and Wada K, ishimine S, Fujisawa N, Kawamori T, Matsuhashi N, Kadowaki T, Ochiai M, Sekihara H, and Nakagama H. Peroxisome proliferator-activated receptor gamma ligands suppress colon carcinogenesis induced by azoxymethane in mice. Gastroenterology. **124**: 361–367. 2003. [Medline]
22. Steffensen IL, Paulsen JE, Eide TJ, and Alexander J. 2-Amino-1-methyl-6-phenylimidazo[4,5-*b*]pyridine increases the numbers of tumors, cystic crypts and aberrant crypt foci in multiple intestinal neoplasia mice. Carcinogenesis. **18**: 1049–1054. 1997. [Medline]
23. Shih CK, Chiang W, and Kuo ML. Effects of adlay on azoxymethane-induced colon carcinogenesis in rats. Food Chem Toxicol. **42**: 1339–1347. 2004. [Medline]
24. Hata K, Yamada Y, Kuno T, Hirose Y, Hara A, Qiang SH, and Mori H. Tumor formation is correlated with expression of β-catenin-accumulated crypts in azoxymethane-induced colon carcinogenesis in mice. Cancer Sci. **95**: 316–320. 2004. [Medline]
25. Holt PR, Mokuolu AO, Distler P, Liu T, and Reddy BS. Regional distribution of carcinogen-induced colonic neoplasia in the rat. Nutr Cancer. **25**: 129–135. 1996. [Medline]
26. Papanikolaou A, Wang QS, Papanikolaou D, Whiteley HE, and Rosenberg DW. Sequential and morphological analyses of aberrant crypt foci formation in mice of differing susceptibility to azoxymethane-induced colon carcinogenesis. Carcinogenesis. **21**: 1567–1572. 2000. [Medline]
27. Femia AP, and Caderni G. Rodent models of colon carcinogenesis for the study of chemopreventive activity of natural products. Planta Med. **74**: 1602–1607. 2008. [Medline]
28. Lance P, and Hamilton SR. Sporadic aberrant crypt foci are not a surrogate endpoint for colorectal adenoma prevention. Cancer Prev Res (Phila). **1**: 4–8. 2008. [Medline]
29. Carter JW, Lancaster HK, Hardman WE, and Cameron IL. Distribution of intestine-associated lymphoid tissue, aberrant crypt foci, and tumors in the large bowel of 1,2-dimethylhydrazine-treated mice. Cancer Res. **54**: 4304–4307. 1994. [Medline]
30. Maskens AP. Histogenesis and growth pattern of 1,2-dimethylhydrazine-induced rat colon adenocarcinoma. Cancer Res. **36**: 1585–1592. 1976. [Medline]
31. Glauert HP, and Weeks JA. Dose- and time-response of colon carcinogenesis in Fischer-344 rats after a single dose of 1,2-dimethylhydrazine. Toxicol Lett. **48**: 283–287. 1989. [Medline]
32. Thorup I. Histomorphological and immunohistochemical characterization of colonic aberrant crypt foci in rats: relationship to growth factor expression. Carcinogenesis. **18**: 465–472. 1997. [Medline]
33. Bird RP, and Pretlow TP. Correspondence re: Giovanna C et al., Effect of dietary carbohydrates on the growth of dysplastic crypt foci in the colon of rats treated with 1,2-dimethylhydrazine. Cancer Res., 51: 3721-3725, 1991. Cancer Res. **52**: 4291–4292. 1992. [Medline]
34. Ochiai M, Watanabe M, Nakanishi M, Taguchi A, Sugimura T, and Nakagama H. Differential staining of dysplastic aberrant crypt foci in the colon facilitates prediction of carcinogenic potentials of chemicals in rats. Cancer Lett. **220**: 67–74. 2005. [Medline]
35. Ochiai M, Ushigome M, Fujiwara K, Ubagai T, Kawamori T, Sugimura T, Nagao M, and Nakagama H. Characterization of dysplastic aberrant crypt foci in the rat colon induced by 2-amino-1-methyl-6-phenylimidazo[4,5-*b*]pyridine. Am J Pathol. **163**: 1607–1614. 2003. [Medline]
36. Paulsen JE, Steffensen IL, Loberg EM, Husoy T, Namork E, and Alexander J. Qualitative and quantitative relationship between dysplastic aberrant crypt foci and tumorigenesis in the Min/+ mouse colon. Cancer Res. **61**: 5010–5015. 2001. [Medline]
37. Kristiansen E, Thorup I, and Meyer O. Influence of different diets on development of DMH-induced aberrant crypt foci and colon tumor incidence in Wistar rats. Nutr Cancer. **23**: 151–159. 1995. [Medline]

38. Otori K, Sugiyama K, Hasebe T, Fukushima S, and Esumi H. Emergence of adenomatous aberrant crypt foci (ACF) from hyperplastic ACF with concomitant increase in cell proliferation. Cancer Res. **55**: 4743–4746. 1995. [Medline]
39. McLellan EA, Medline A, and Bird RP. Sequential analyses of the growth and morphological characteristics of aberrant crypt foci: putative preneoplastic lesions. Cancer Res. **51**: 5270–5274. 1991. [Medline]
40. Yamashita N, Minamoto T, Ochiai A, Onda M, and Esumi H. Frequent and characteristic K-ras activation in aberrant crypt foci of colon. Is there preference among K-ras mutants for malignant progression? Cancer. **75**: 1527–1533. 1995. [Medline]
41. Pretlow TP, Roukhadze EV, O'Riordan MA, Chan JC, Amini SB, and Stellato TA. Carcinoembryonic antigen in human colonic aberrant crypt foci. Gastroenterology. **107**: 1719–1725. 1994. [Medline]
42. Paulsen JE, Loberg EM, Olstorn HB, Knutsen H, Steffensen IL, and Alexander J. Flat dysplastic aberrant crypt foci are related to tumorigenesis in the colon of azoxymethane-treated rat. Cancer Res. **65**: 121–129. 2005. [Medline]
43. Yamada Y, Yoshimi N, Hirose Y, Kawabata K, Matsunaga K, Shimizu M, Hara A, and Mori H. Frequent *β-catenin* gene mutations and accumulations of the protein in the putative preneoplastic lesions lacking macroscopic aberrant crypt foci appearance, in rat colon carcinogenesis. Cancer Res. **60**: 3323–3327. 2000. [Medline]
44. Yamada Y, Yoshimi N, Hirose Y, Matsunaga K, Katayama M, Sakata K, Shimizu M, Kuno T, and Mori H. Sequential analysis of morphological and biological properties of β-catenin-accumulated crypts, provable premalignant lesions independent of aberrant crypt foci in rat colon carcinogenesis. Cancer Res. **61**: 1874–1878. 2001. [Medline]
45. Caderni G, Femia AP, Giannini A, Favuzza A, Luceri C, Salvadori M, and Dolara P. Identification of mucin-depleted foci in the unsectioned colon of azoxymethane-treated rats: correlation with carcinogenesis. Cancer Res. **63**: 2388–2392. 2003. [Medline]
46. Femia AP, Dolara P, Giannini A, Salvadori M, Biggeri A, and Caderni G. Frequent mutation of Apc gene in rat colon tumors and mucin-depleted foci, preneoplastic lesions in experimental colon carcinogenesis. Cancer Res. **67**: 445–449. 2007. [Medline]
47. Femia AP, Bendinelli B, Giannini A, Salvadori M, Pinzani P, Dolara P, and Caderni G. Mucin-depleted foci have beta-catenin gene mutations, altered expression of its protein, and are dose- and time-dependent in the colon of 1,2-dimethylhydrazine-treated rats. Int J Cancer. **116**: 9–15. 2005. [Medline]
48. Femia AP, Tarquini E, Salvadori M, Ferri S, Giannini A, Dolara P, and Caderni G. K-ras mutations and mucin profile in preneoplastic lesions and colon tumors induced in rats by 1,2-dimethylhydrazine. Int J Cancer. **122**: 117–123. 2008. [Medline]
49. Femia AP, Dolara P, and Caderni G. Mucin-depleted foci (MDF) in the colon of rats treated with azoxymethane (AOM) are useful biomarkers for colon carcinogenesis. Carcinogenesis. **25**: 277–281. 2004. [Medline]
50. Femia AP, Giannini A, Fazi M, and Tarquini E. salvadori M, Roncucci L, Tonelli F, and Dolara P, Caderni G. Identification of mucin depleted foci in the human colon. Cancer Prev Res (Phila). **1**: 562–567. 2008. [Medline]
51. Sakai E, Morioka T, Yamada E, Ohkubo H, Higurashi T, Hosono K, Endo H, Takahashi H, Takamatsu R, Cui C, Shinozawa M, Araike M, Samura H, Nishimaki T, Nakajima A, and Yoshimi N. Identification of preneoplastic lesions as mucin-depleted foci in patients with sporadic colorectal cancer. Cancer Sci. **103**: 144–149. 2012. [Medline]

Cancer Science
The official journal of the Japanese Cancer Association

Purple corn color inhibition of prostate carcinogenesis by targeting cell growth pathways

Ne Long,[1] Shugo Suzuki,[1] Shinya Sato,[1] Aya Naiki-Ito,[1] Keisuke Sakatani,[2] Tomoyuki Shirai[1,3] and Satoru Takahashi[1,4]

[1]Department of Experimental Pathology and Tumor Biology, Nagoya City University Graduate School of Medical Sciences, Nagoya; [2]Food Color Laboratory, San-Ei Gen F.F.I., Inc., Osaka; [3]Nagoya City Rehabilitation Center, Nagoya, Japan

(Received September 24, 2012/Revised November 5, 2012/Accepted November 20, 2012/Accepted manuscript online November 30, 2012/Article first published online January 20, 2013)

Purple corn color is a widely used food colorant that was reported to have attenuating effects on hypertension, diabetes, and to have anti-cancer effects on colon and breast cancer. Our study is the first on its possible chemoprevention effects against prostate cancer. For this purpose an androgen-dependent prostate cancer cell line, LNCaP, was used to examine effects *in vitro*. Purple corn color inhibited the proliferation of LNCaP cells by decreasing the expression of Cyclin D1 and inhibiting the G1 stage of the cell cycle. Thirty-six male transgenic rats for adenocarcinoma of prostate were fed basic diet or diet with purple corn color for 8 weeks. Purple corn color decreased the incidence of adenocarcinoma in the lateral prostate and slowed down the progression of prostate cancer. A lower Ki67 positive rate, a decrease of the expression of Cyclin D1, and downregulation of the activation of Erk1/2 and p38 MAPK were observed in the group consuming purple corn color in the diet. Since purple corn color is a mixture, determining its active component should help in the understanding and usage of purple corn color for prostate cancer chemoprevention. Therefore, the three major anthocyanins in purple corn color, cyanidin-3-glucoside, pelargonidin-3-glucoside and peonidin-3-glucoside, were tested with LNCaP cells. The results suggested that cyanidin-3-glucoside and pelargonidin-3-glucoside are the active compounds. (*Cancer Sci* 2013; 104: 298–303)

Cancer is a major public health problem in developed and some developing countries. In 2012, prostate cancer (PCa) was estimated to be the No.1 cause of new cancer cases in males and the second highest cause of cancer related deaths in the USA,[1] and PCa is rapidly increasing in Asia. Although considerable effort has been expended on searching for early screening markers and curing PCa, the main treatment remains androgen ablation therapy, which was developed in the early 1940s.[2,3] However, even though more than 80% of PCa respond to this therapy, almost all of these cases relapse in less than a decade and become refractory to treatment.[3] Brachytherapy, radiotherapy, and prostatectomy of PCa prior to metastasis can affect a cure, but these procedures can dramatically alter the quality-of-life of the patient.[4,5] Therefore, prevention of PCa is especially important.

The field of chemoprevention, using natural or laboratory-made substances to prevent cancer, has become increasingly studied in recent years. Researchers have investigated numerous chemicals that may have chemopreventive effects on PCa *in vitro* and *in vivo*. Three large-scale randomized, controlled clinical trials have been conducted: the SELECT trial found that neither selenium nor Vitamin E reduced the risk of PCa in healthy men at average risk;[6] the PCPT trial found that finasteride, a 5α-reductase inhibitor, reduced the risk of PCa of Gleason 6 or less, whereas there was an increased risk of high grade disease with Gleason 7 or more;[7] the REDUCE trial also encountered similar difficulties with dutasteride, another 5 α-reductase inhibitor.[8] Therefore, the search for an appropriate chemopreventor for PCa needs to be continued.

Purple corn has a long history as a food product. Nowadays its color is widely used as a food colorant in Japan. Previous studies have provided evidence that purple corn color (PCC) has anti-cancer effects on colon and breast cancer.[9,10] It also has attenuating effects on some life style diseases, for example, hypertension, hyperglycemia, and diabetes.[11,12] The present study was conducted as an initial investigation on PCC's effects on PCa. As a result we found that PCC inhibited the proliferation of the androgen-dependent cell line LNCaP *in vitro* and inhibited prostate carcinogenesis *in vivo* in the Transgenic Rat for Adenocarcinoma of Prostate (TRAP) model. The TRAP rat model, in which expression of the Simian virus 40 T antigen is under control of the probasin gene promoter, was established in our laboratory. These animals develop high-grade prostatic intraepithelial neoplasia (HG-PIN) and well-differentiated adenocarcinomas with high incidence in all prostate lobes at 15 weeks of age, all lesions being completely androgen-dependent.[13,14] The model provides an ideal tool to gain insights into possible mechanisms of PCa prevention in relatively short-term studies.[15–19]

Purple corn color is a mixture, which contains several anthocynins. To determine its active component, the three major anthocyanins in PCC, cyanidin-3-glucoside (C3G), pelargonidin-3-glucoside (Pg3G) and peonidin-3-glucoside (P3G), were tested using LNCaP cells. By comparing the effects of these anthocyanins to the effect of the mixture, we found that C3G and Pg3G are the active compounds.

To our knowledge, the present study provides the first evidence that PCC inhibits prostate carcinogenesis in a rat model closely mimicking the human disease. The clues obtained as to the molecular basis of action are of critical importance as first steps towards human clinical trials.

Materials and Methods

Chemicals, reagents, plasmids and cell line. Purple corn color was provided by San-Ei Gen F.F.I. (Osaka, Japan). Lot No. 100413, anthocyanin concentration 12.5% was used for the *in vitro* study. Lot No. 110418, anthocyanin concentration 20.9% was used for the *in vivo* study. C3G (Cyanidin-3-O-glucoside chloride) and P3G (Peonidin-3-O-glucoside chloride) were purchased from Tokiwa Phytochemical (Chiba, Japan). Pg3G (Pelargonidin-3-O-glucoside chloride) was purchased from Extrasynthese (Genay Cedex, France). The chemical structures of C3G, P3G and Pg3G are shown in Supplementary

[4]To whom correspondence should be addressed.
E-mail: sattak@med.nagoya-cu.ac.jp

doi: 10.1111/cas.12078
© 2012 Japanese Cancer Association

Figure S1. The LNCaP human PCa cell line (androgen-dependent) was from the American Type Culture Collection (Manassas, VA, USA). The pGL3-PSA luciferase expression vector (pGL3/PSA-Luc) was donated by Dr Chawnshang Chang, University of Rochester Medical Center.

Animals. Male heterozygous TRAP rats with a Sprague–Dawley genetic background were used in the present study. They housed three animals per cage on wood-chip bedding in an air-conditioned animal room at 23 ± 2°C and 50 ± 10% humidity. Food and tap water were available *ad libitum*. The Institutional Animal Care and Use Committees of the Nagoya City University (Nagoya, Japan) specifically approved this study.

Experimental protocol. A total of 36 heterozygous male TRAP rats at 6 weeks of age were randomly divided into three groups. Rats in the control group (n = 13) received powdered basal diet (Oriental MF, Oriental Yeast, Tokyo, Japan). The rats in the other two groups received 0.1% (n = 12) or 1% PCC (n = 11) in the diet for 8 weeks. At the end of week 8, the rats were killed under deep anesthesia. Each prostate was removed and halves of the ventral and lateral lobes were immediately frozen in liquid nitrogen and stored at −80°C until processed; the remaining prostates was fixed in 10% neutral buffered formalin, embedded in paraffin, and sectioned. Testosterone and estrogen levels in the serum were analyzed by radioimmunoassay by SRL (Tokyo, Japan). All experiments were performed under protocols approved by the Institutional Animal Care and Use Committee of Nagoya City University Graduate School of Medical Sciences.

Assessment of prostate neoplastic lesion development. Neoplastic lesions in the prostate glands of TRAP rats were evaluated as previously described.[19] Briefly, neoplastic lesions were classified into three types: low-grade prostatic intraepithelial neoplasia (LG-PIN), HG-PIN and adenocarcinoma. The relative numbers of acini with the histological characteristics of each type, that is, LG-PIN, HG-PIN and adenocarcinoma, were quantified with reference to the total acini in each prostatic lobe.

Immunoblot analysis. The immunoblotting analysis was performed as described previously.[19] Briefly, LNCaP cells or frozen ventral prostate tissues were homogenized in radioimmunoprecipitation assay buffer (150 mM NaCl, 50 mM Tris –HCl [pH 8.0], 1% NP-40, 0.5% sodium deoxycholate, 0.1% SDS, 1 mM phenylmethylsulphonyl fluoride, 1 mM sodium orthovanadate, and protease inhibitor cocktail [Complete, Roche, Mannheim, Germany]) and subjected to immunoblot analysis using standard techniques. The antibodies used were Cyclin D1 and androgen receptor (Santa Cruz Biotechnology, Santa Cruz, CA, USA), cleaved caspase 3, cleaved caspase 7, Erk1/2, phospho-Erk1/2, p38 MAPK and phospho-p38 MAPK (Cell Signaling Technology, Boston, MA, USA), prostate-specific antigen (DAKO, Tokyo, Japan) and β-actin (Sigma-Aldrich, St. Louis, MO, USA). The density of the bands was semi-quantified using ImageJ (version 1.42q, National Institute of Health, Bethesda, MD, USA).

Immunohistochemistry. Deparaffinized sections were incubated with antibodies for Ki-67 (Novocastra Laboratories, Newcastle, UK) and SV40 T antigen (Santa Cruz Biotechnologies). Apoptotic cells in the prostate were detected using an *In Situ* Apoptosis Detection kit (TUNEL method) according to the manufacturer's instructions (Takara Bio, Ohtsu, Japan). Labeling indices were determined as the positive percentage for Ki-67 or TUNEL by randomly picking eight fields of view in the whole ventral/lateral prostate and counting over 1000 prostate epithelial cells under a microscope at high magnification.

Cell proliferation assay. Cell proliferation of LNCaP cells was assessed by manual counting under trypan blue staining. Briefly, LNCaP cells were seeded in 96-well plates at 10 000 cells/well in 200 μL of RPMI media; PCC, C3G, Pg3G or P3G were added 24 h after seeding and the cells were incubated for 72 h; and the cells were removed from the plate with trypsin-EDTA and counted.

RNA extraction, cDNA preparation, and quantitative real-time PCR. Total RNAs of LNCaP cells or frozen prostate tissue was isolated using an RNeasy Mini kit (Qiagen, Valencia, CA, USA) and reverse-transcribed with the Thermoscript first-strand synthesis system (Invitrogen Corporation, Carlsbad, CA, USA). Real-time RT-PCR was performed using Syber Premix Ex Taq II (Takara) in a LightCycler (Roche Diagnostics GmbH). The primers used were: human GAPDH, 60°C, 5′-AACGGATTTGGTCGTATTGG-3′ and 5′-CATACTTCTCATGGTTCACA-3′; human Cyclin D1, 60°C, 5′-CCGAGAAGCTGTGCATCTAC-3′ and 5′-CAGGTTCAGGCCTTGCACTG-3′; rat GAPDH, 59°C, 5′-GAATGGGAAGCTGGTCATCA-3′ and 5′-TGGATGCAGGGATGATGTTC-3′; rat probasin, 60°C, 5′-ACTTCCGTCGCATTGAGTGT-3′ and 5′-GTAAACGTCTTGGGATCTCC-3′; rat GK11, 59°C, 5′-GCAGCACCAAACCCCTGGAT-3′ and 5′-TGAGATCTGTCACCTTCTCA-3′.

Cell cycle analysis. LNCaP cells were seeded in 6-well plates at 150 000 cells/well. Purple corn color, C3G or Pg3G were added 24 h after seeding, incubated for 72 h, collected and analyzed with propidium iodide (Guava cell cycle reagent; Guava Technologies, Hayward, CA, USA) according to the Guava Cell Cycle Assay protocol. The cell cycle phase distribution was determined on a Guava PCA Instrument using CytoSoft Software.

Reporter gene assays. LNCaP cells were transfected with the pGL3/PSA-Luc using Nucleofector II. 24 h later, 5 nM DHT and/or PCC were added. After 48 h incubation, the cells were lysed with the buffer supplied in the kit. Luciferase assays were conducted using the dual-luciferase reporter assay system (Promega, Madison, WI, USA), and the phRL-TK vector (Promega) as an internal control, according to the manufacturer's protocol. Data shown are means and SD of four independent data points.

Statistical analysis. All data presented are mean ± SD values. Statistical comparisons were performed with one-way ANOVA followed by Dunnett's test. Correlations were assessed by Spearman correlation coefficient analysis. A P-value of < 0.05 was considered to be significant. All statistical analyses were performed using GraphPad Prism 5 (GraphPad Software, La Jolla, CA, USA).

Results

PCC inhibition of LNCaP proliferation and slowing of the cell cycle. When the androgen-dependent cell line LNCaP was incubated with increasing levels of PCC for 72 h, the proliferation of the cells was inhibited in a dose-dependent manner (Fig. 1A). Cell cycle analysis showed that PCC increased the proportion of cells in G0/G1 slightly but significantly (Fig. 1B). Western blotting showed a 15–30% decrease in the protein level of Cyclin D1 in the PCC treated cells (Fig. 1C), and reverse-transcription PCR also showed that the mRNA level of Cyclin D1 was significantly decreased by PCC (Fig. 1D). Purple corn color did not affect androgen receptor (AR) expression, but PSA expression was dramatically decreased (Fig. 1C). Since the PSA gene is a target of AR, we used a luciferase assay to examine the influence of PCC on the activity of the PSA promoter. Purple corn color inhibited functional AR transcriptional activity in a dose-dependent manner (Fig. S2).

No toxic effects of PCC were observed in the TRAP rat model. Body weights, relative organ weights (ventral prostate, liver and kidney), and food consumption were not affected by administration of PCC in the diet to TRAP rats (Table S1). The average PCC intakes were 25 mg/rat per day and 267 mg

© 2012 Japanese Cancer Association

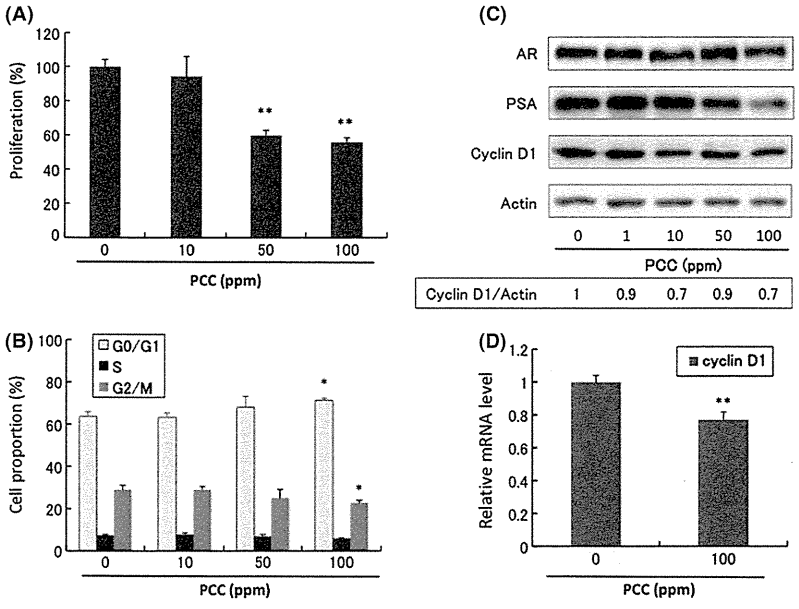

Fig. 1. Effects of purple corn color (PCC) on LNCaP cells. (A) Inhibitory effects on LNCaP cell proliferation (72 h) (n = 3). (B) Effects on the cell cycle of LNCaP cells (n = 3). (C) Protein changes assessed by Western blotting analysis of LNCaP cells after incubation with PCC for 72 h. The density of the bands of Cyclin D1 and actin were semi-quantified by ImageJ. (D) mRNA levels of Cyclin D1 analyzed by reverse-transcription polymerase chain reaction (n = 3). *P < 0.05; **P < 0.01; ***P < 0.001.

/rat per day for the 0.1% and 1% PCC groups (Table S1). Purple corn color did not have any effect on the serum levels of testosterone or estradiol (Table S1).

PCC inhibition of prostate carcinogenesis in the TRAP rat model. With the expression of SV40T antigen under the control of AR, TRAP rats developed prostate cancer with high incidence. In the end of the experiment, all the acini in both ventral and lateral prostate of TRAP rats had developed precancerous or cancerous lesions. Lesions were divided into three stages: LG-PIN, HG-PIN, and adenocarcinoma (Fig. S3). The total percentage of LG-PIN, HG-PIN and adenocarcinoma is 100%. In this study, adenocarcinomas were observed in ventral prostate of all the rats, that is, the incidence of adenocarcinoma was 100% in all three groups. However, the rats consuming PCC had a lower percentage of adenocarcinoma and a higher percentage of LG-PIN (Table 1), which suggests that PCC retarded the progression of PCa and more acini lesions remained in the relatively benign LG-PIN stage. The increased LG-PIN percentage and decreased adenocarcinoma percentage showed a strong correlation to the dose of PCC. In the lateral prostate, we also observed this retardation of PCa progression. Of critical importance in this study is that PCC also significantly decreased the incidence of adenocarcinoma in the lateral prostate (Table 1). These results suggest that PCC inhibited tumorigenesis in the prostates of TRAP rats.

PCC inhibition of the cell growth pathways in the TRAP rat model. Carcinogenesis in the TRAP rat is induced by SV40T antigen expressed under the control of the probasin promoter, which is regulated by the AR. Since PCC downregulated AR activity *in vitro*, we examined whether SV40T expression was downregulated by PCC. Immunohistochemical analysis showed that there was no overt inhibition of SV40T expression by PCC (Fig. 2A,B). We used RT-PCR to examine mRNA levels in the VP of the androgen responsive genes probasin and GK11, an ortholog of human PSA. These results also indicated that AR activity was not inhibited by PCC (Fig. 2C).

Figure 3A shows that the Ki67 index was decreased by PCC in both VP and LP. On the other hand, the TUNEL staining index was not affected by PCC (Fig. 3B), in agreement with our *in vitro* studies in which no apoptosis was observed (data not shown).

Immunoblotting demonstrated factors involved in cell growth pathways, Erk1/2 and p38 MAPK phosphorylation and Cyclin D1, to be downregulated by PCC. In agreement with the results of TUNEL staining, PCC had no affect on the levels of cleaved caspases 3 or 7 (Fig. 3C).

Search for active compounds in PCC. The compounds that give PCC its purple color are anthocyanins. C3G, Pg3G and P3G are the three major components of PCC. When their effects on LNCaP cells were tested, C3G and Pg3G dose-dependently inhibited the proliferation of LNCaP cells, while P3G had no effect (Fig. 4A). The differences of the chemical structures of these three chemicals (Fig. S1) suggest that the hydroxyl radical may play an important role in the inhibitory activity on PCa. Both C3G and Pg3G upregulated AR expression. However, PSA expression, an indicator of AR activity, remained the same (Fig. 4B). This effect on AR activity is in contrast to the effect of PCC *in vitro* but similar to that *in vivo*. Both C3G and Pg3G decreased the expression of Cyclin D1 (Fig. 4C), while increasing the proportion of cells in G0/G1 (Fig. 4D,E), again in line with the PCC effect.

Discussion

Purple corn color is reported to have anti-cancer effect on colon and breast cancer,[9,10] and it also has attenuating effects on some life style diseases, for example, hypertension, hyperglycemia, and diabetes.[11,12] Like breast cancer, PCa is hormone-related. Prostate cancer is also closely associated with a high-fat diet.[20,21] Finally, in the TRAP model, hypertension is positively associated with PCa development.[22] Therefore, we investigated the possibility that PCC could have inhibitory effects on PCa. The results of our experiments, both *in vitro* and *in vivo*, supported this hypothesis. Purple corn color not only showed antiproliferative effects on an androgen-dependent PCa cell line, it also inhibited prostate carcinogenesis *in vivo*. Importantly, dietary PCC did not have any observable toxic effects: there were no significant changes in the final body weights or relative liver or kidney weights in rats fed PCC in their diets. This suggests that PCC could be used as a long-term dietary supplement for chemoprevention of PCa. The success of PCC in the TRAP

doi: 10.1111/cas.12078
© 2012 Japanese Cancer Association

Table 1. Quantitative evaluation of neoplastic lesions in prostates of TRAP rats treated with PCC

	No. of animal	Incidence of adenocarcinoma	Proportion of acini in different stages of carcinogenesis (%)		
			LG-PIN	HG-PIN	Adenocarcinoma
Ventral prostate					
Control	13	13 (100%)	4.4 ± 2.8	89.2 ± 3.5	6.4 ± 4.0
0.1% PCC	12	12 (100%)	5.9 ± 3.4**	90.6 ± 3.8	3.5 ± 1.7***
1% PCC	11	11 (100%)	9.1 ± 3.9**	88.2 ± 3.4	2.7 ± 2.0***
Lateral prostate					
Control	13	12 (92%)	24.7 ± 12.4	72.8 ± 11.7	2.5 ± 2.8
0.1% PCC	12	7 (58%)	17.8 ± 5.6	81.2 ± 5.6	1.0 ± 1.0**
1% PCC	11	3 (27%)*	21.1 ± 6.8	78.0 ± 6.2	0.9 ± 1.6**

AC, adenocarcinoma; HG, high grade; LG-PIN, low grade prostatic intraepithelial neoplasia. *P < 0.01 versus control (Dunnett's test). **P < 0.01 and ***P < 0.001 versus control, respectively (Spearman's rank correlation coefficient analysis).

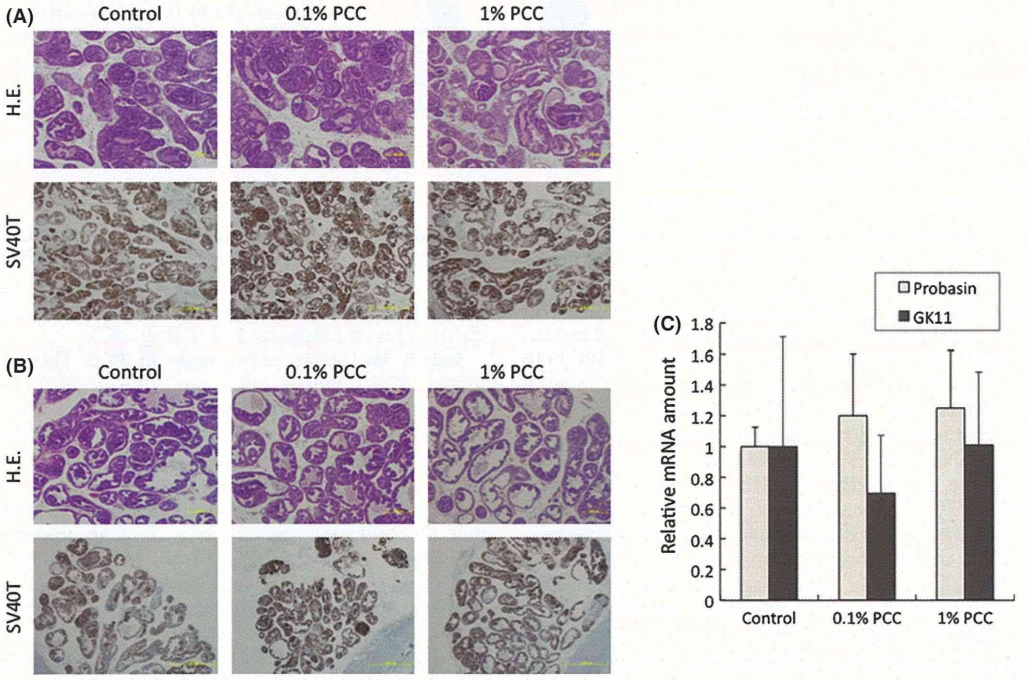

Fig. 2. Purple corn color (PCC)-mediated inhibition of carcinogenesis is not due to down regulation of androgen receptor (AR) activity. (A) H&E staining (4 × magnification) and SV40T antigen expression (4 × magnification) in the ventral prostate. (B) H&E staining (4 × magnification) and SV40T antigen expression (4 × magnification) in the lateral prostate. (C) mRNA of the ventral prostate was used for reverse-transcription polymerase chain reaction. mRNA levels of probasin and GK11 (the rat ortholog of human PSA), which are AR target genes, were checked. Scale bars, 500 μm.

rat model demonstrates that PCC may inhibit prostate carcinogenesis not only in a simple *in vitro* tissue culture system but also in the complex system of living experimental animals.

To date, an enormous effort has been made to find means to prevent PCa, but an ideal chemopreventor active by itself has yet to be found. The trend has therefore been to put chemicals that target different pathways together to form a "cocktail" that would be more effective. Our laboratory has been focused on looking for PCa chemopreventors. We previously reported that resveratrol could inhibit PCa genesis by targeting the AR pathway,[19] while γ-tocopherol exerts inhibitory effects though activation of caspase-signaling.[23] In the present study, we found that PCC targets cell growth. A reasonable expectation is that combining PCC, resveratrol and γ-tocopherol could have a greater effect than using any of the compounds singly. This is a direction for future studies.

To better understand the chemopreventive effects of PCC on PCa, identifying the active components is essential. Cell proliferation assays here indicated that both C3G and Pg3G dose-dependently inhibited the growth of LNCaP. Similarly to PCC, both C3G and Pg3G decreased the expression of Cyclin D1 and increased the percentage of LNCaP cells in G0/G1. The increased percentage of cells in G0/G1 was about 1.1 times compared to the control. Importantly, the cell proliferation was inhibited by approximately 50%. This suggests that while the effect of C3G and Pg3G on the cell proliferation is rather small, the cumulative effect over time can be substantial. Intriguingly, although the PCC mixture downregulated AR activity, C3G and Pg3G did not show the same effect. Notably, PCC inhibited carcinogenesis in the TRAP model without

© 2012 Japanese Cancer Association

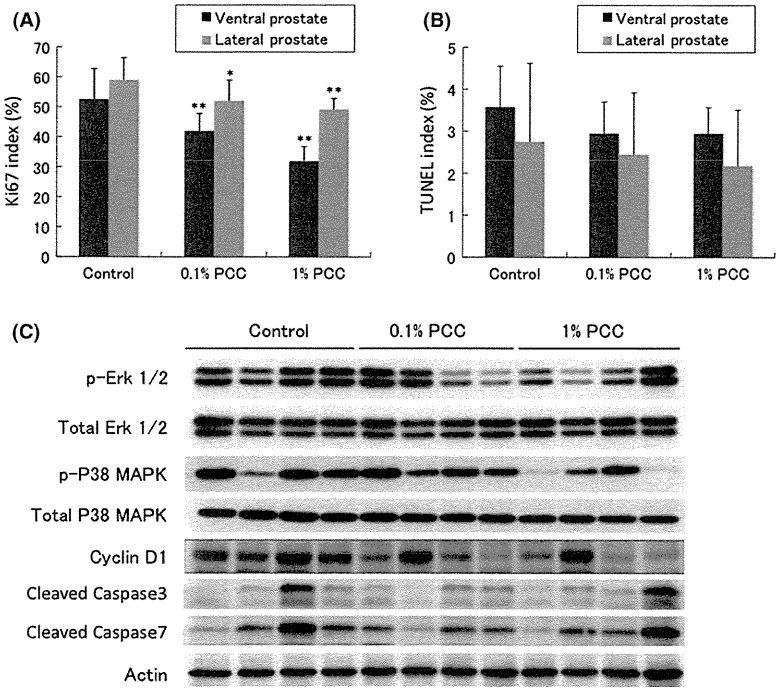

Fig. 3. Effects of purple corn color (PCC) on Ki67 and terminal deoxynucleotidyl transferase-mediated dUTP nick end labeling (TUNEL) indices in the prostate. (A) Purple corn color decreased the Ki67 index significantly in both the ventral and lateral prostate (samples from all the rats were used for analysis). (B) Purple corn color did not affect the TUNEL index in either the ventral or lateral prostate (samples from all the rats were used for analysis). (C) Western blot of proteins related to cell growth and apoptosis using samples from the ventral prostate.

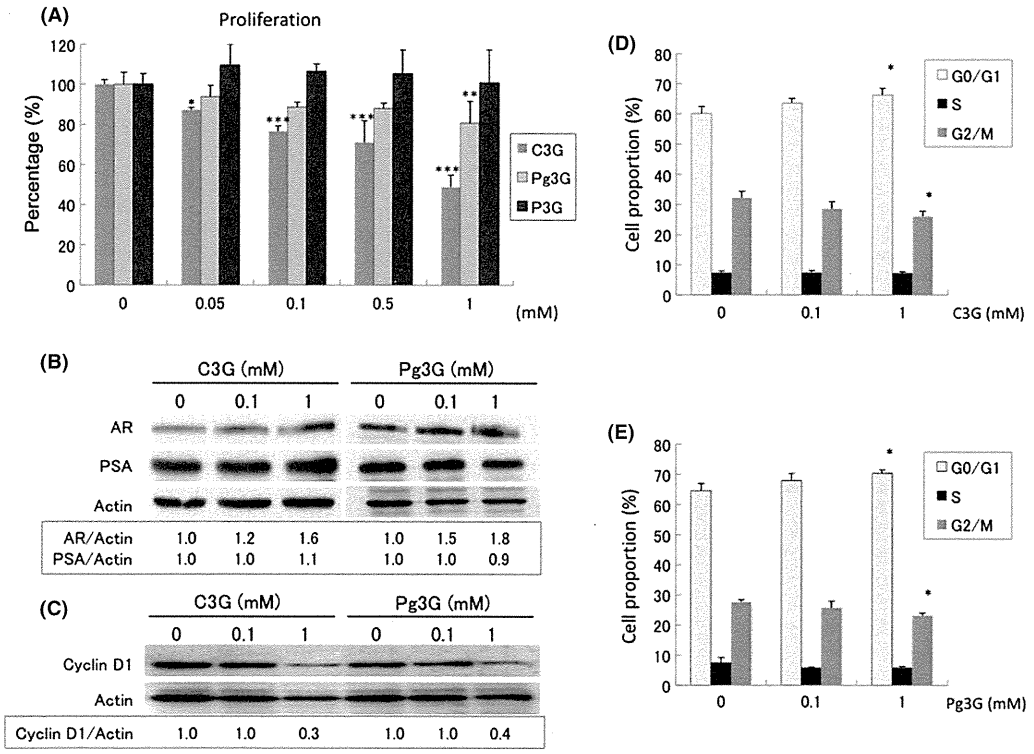

Fig. 4. Anthocyanins in the purple corn color (PCC) mixture, cyanidin-3-glucoside (C3G), pelargonidin-3-glucoside (Pg3G) and peonidin-3-glucoside (P3G), were tested using LNCaP cells. (A) Effects of C3G, Pg3G and P3G on LNCaP cell proliferation. (B,C) Findings of Western blotting. The density of the bands of androgen receptor (AR), PSA and actin were semi-quantified by ImageJ. (D) Effects of C3G on the cell cycle of LNCaP cells. (E) Effects of Pg3G on the cell cycle of LNCaP cells. $*P < 0.05$; $**P < 0.01$; $***P < 0.001$.

downregulating AR activity. Therefore, it is likely that PCC does not inhibit PCa through downregulation of AR. The downregulation observed with the PCC mixture *in vitro* might be a byproduct of other compounds. Taken together, these results suggest that C3G and Pg3G are the probable active compounds contained in PCC.

doi: 10.1111/cas.12078
© 2012 Japanese Cancer Association